Mantle plumes and their role in Earth processes

Anthony A. P. Koppers[1]✉, *Thorsten W. Becker*[2], *Matthew G. Jackson*[3], *Kevin Konrad*[1,4], *R. Dietmar Müller*[5], *Barbara Romanowicz*[6,7,8], *Bernhard Steinberger*[9,10] *and Joanne M. Whittaker*[11]

Abstract | The existence of mantle plumes was first proposed in the 1970s to explain intra-plate, hotspot volcanism, yet owing to difficulties in resolving mantle upwellings with geophysical images and discrepancies in interpretations of geochemical and geochronological data, the origin, dynamics and composition of plumes and their links to plate tectonics are still contested. In this Review, we discuss progress in seismic imaging, mantle flow modelling, plate tectonic reconstructions and geochemical analyses that have led to a more detailed understanding of mantle plumes. Observations suggest plumes could be both thermal and chemical in nature, can attain complex and broad shapes, and that more than 18 plumes might be rooted in regions of the lowermost mantle. The case for a deep mantle origin is strengthened by the geochemistry of hotspot volcanoes that provide evidence for entrainment of deeply recycled subducted components, primordial mantle domains and, potentially, materials from Earth's core. Deep mantle plumes often appear deflected by large-scale mantle flow, resulting in hotspot motions required to resolve past tectonic plate motions. Future research requires improvements in resolution of seismic tomography to better visualize deep mantle plume structures at smaller than 100-km scales. Concerted multi-proxy geochemical and dating efforts are also needed to better resolve spatiotemporal and chemical evolutions of long-lived mantle plumes.

Hotspot
Region of intra-plate volcanism that forms an age-progressive volcanic chain (like Hawaii) or a region of excessive volcanism along plate boundaries (like Iceland), with temperatures exceeding that of ambient asthenospheric mantle by ~100 °C or more.

Large igneous provinces
(LIPs). Extremely large accumulations of intrusive and extrusive volcanic rocks (areal extents >0.1 million km^2 with volumes >0.1 million km^3) deposited over a short geological period of time, often in less than 1 million years.

✉e-mail: anthony.koppers@oregonstate.edu

https://doi.org/10.1038/s43017-021-00168-6

Narrow mantle upwellings, or plumes, are an integral part of Earth's convection system, yet many controversies have surrounded mantle plumes since the idea was first invoked[1]. Where the plate tectonic revolution in the 1960s provided an explanation for volcanism at plate boundaries, it did not provide a model for the occurrence of volcanism in the middle of plates. However, in 1963, it was the northwest-oriented lineament of volcanic islands forming the Hawaiian archipelago that could be explained by a rigid tectonic plate moving over a hotspot in Earth's asthenosphere, allowing for intra-plate magma production[2]. Almost a decade later, in 1971, it was hypothesized that such a hotspot could form above a vertical, narrow, hot mantle plume rising from the deep mantle[1]. In these initial models, mantle plumes were defined as narrow thermal upwellings[1] with a wide ~1,000-km plume head, followed by a thinner ~100-km tail[3,4]. The deep mantle sources of plumes were later connected to the recycling of old oceanic lithosphere (and sediments) conveyed to Earth's deep interior via subduction over the course of hundreds of millions to billions of years[5–7], thus, completing the convection cycle. How many mantle plumes exist, at what depth in the mantle they originate, their longevity and petrological make-up, the relationships between various geophysical and geochemical observations, and the dynamics and shapes of plumes are still hotly contested, leaving numerous open questions in the understanding of Earth's interior.

To date, it is understood that mantle plumes could start as deep as the core–mantle boundary at roughly 2,900-km depth[8–15]. These plumes are also thought to have temperatures in excess of ~100–300 °C compared with the ambient mantle[16–21] and require tens of millions of years to ascend to the base of Earth's lithosphere, where they form hotspots (FIG. 1a). Computer modelling and laboratory experiments, however, have shown how entrainment of chemical heterogeneity (FIG. 1b) may change key characteristics of plume conduits, for example, by inclusion of recycled subducted ocean crust[22–26]. As a result, most plumes are now considered thermochemical plumes rather than purely thermal plumes, and are thought to have more intricate structures and broader shapes. At asthenospheric depths, the ascending plumes can exceed the pressure-dependent melting temperature for mantle rocks, leading to partial melting, resulting in widespread magmatism that creates large igneous provinces (LIPs) and age-progressive volcanic hotspot trails[27,28]. Intra-plate hotpot volcanism,

Key points

- Thermochemical mantle plumes are an integral part of Earth's dynamic interior.
- More than 18 mantle plumes appear to originate from the deepest regions in Earth's mantle.
- Mantle plumes influence surface processes, including continental break-up and mass extinctions.
- The location of two large low-seismic-velocity provinces in the lowermost mantle can be associated with most present-day hotspots and ancient large igneous provinces.
- Individual plume motions are required to resolve changes in absolute plate tectonic motions.
- Mantle plumes are geochemically heterogeneous, incorporating deeply recycled subducted components, primordial mantle domains and, potentially, materials from Earth's core.

Large low-shear-velocity provinces
(LLSVPs). A large region (several thousand kilometres in size) of low shear velocity (a few percent lower than average) in the lowermost few hundreds of kilometres of the mantle. There are two of them, beneath Africa and the Pacific.

Hadean
Geologic eon in Earth history, starting with Earth's accretion about 4.567 billion years ago and ending 4 billion years ago at the beginning of the Archaean.

Core–mantle boundary
Boundary between the liquid metal outer core and the mostly solid lower mantle at ~2,891-km depth.

660-km Seismic discontinuity
Seismic discontinuity corresponding to a solid–solid phase transition in the mantle at ~660-km depth.

therefore, provides a unique means of sampling deep mantle plumes, providing key insights into the convective scales and physical conditions of Earth's interior and the chemical evolution of the mantle over billions of years of Earth history[7,16,29,30].

Studies of hotspot volcanoes and mantle plumes also provide an understanding of the broader interplay with deep mantle superstructures, mantle convection, plate tectonics and surface processes. For example, it has been hypothesized that large-scale mantle flow driven by slabs, many of which are subducted to the deep lower mantle and piled up into slab graveyards[11,31–35], will trigger plumes, characteristically above large low-shear-velocity provinces (LLSVPs), where seismic velocities are several percent lower than in surrounding regions[36–42], or focused along their edges[11,13,43,44]. These processes are all part of global elemental cycles governed by mantle convection and, therefore, mantle plumes possibly sample of a variety of global-scale geochemical reservoirs, including ancient mantle domains from Hadean times and a variety of deeply recycled crustal reservoirs[5–7,45–47]. Plumes impinging on Earth's lithosphere might also initiate rifts in continents, aiding in continental break-up and the formation of new ocean basins[48–51]. Ultimately, mantle plumes are able to produce extensive volcanism on Earth's surface, causing major perturbations in its environment and in ocean chemistry, leading to climate change and possibly triggering mass extinctions[52–54].

Author addresses

[1]College of Earth, Ocean, and Atmospheric Sciences, Oregon State University, Corvallis, OR, USA.
[2]Institute for Geophysics and Department of Geological Sciences, Jackson School of Geosciences, The University of Texas at Austin, Austin, TX, USA.
[3]Department of Earth Science, University of California, Santa Barbara, Santa Barbara, CA, USA.
[4]Department of Geoscience, University of Nevada, Las Vegas, Las Vegas, NV, USA.
[5]EarthByte Group, School of Geosciences, The University of Sydney, Sydney, NSW, Australia.
[6]Department of Earth and Planetary Science, University of California, Berkeley, Berkeley, CA, USA.
[7]Collège de France, Paris, France.
[8]Institut de Physique du Globe de Paris, Paris, France.
[9]Helmholtz Centre Potsdam, GFZ German Research Centre for Geosciences, Potsdam, Germany.
[10]Centre for Earth Evolution and Dynamics (CEED), University of Oslo, Oslo, Norway.
[11]Institute for Marine and Antarctic Studies, University of Tasmania, Hobart, TAS, Australia.

However, the dynamics of mantle plumes and their relation to mantle convection and the formation of hotspots in the shallow asthenosphere are still debated. For example, it is unclear whether hotspots are formed by broad upwellings of thousand(s)-kilometre scale triggered by passive return flow from subducting slabs[55,56] or by narrower upwellings of hundred(s)-kilometre scale that are actively rising from a thermal boundary layer in the form of plume-like conduits[25,57–59]. Whether all plumes form either somewhere near the core–mantle boundary or in the upper mantle above the 660-km seismic discontinuity in relation to subduction-driven convection or the ponding of lower mantle plumes is also still debated[28,60–64]. These differences are important in deciphering to what extent there is a separate convectional regime in the upper mantle, besides whole-mantle convection.

Furthermore, the observation that some near-surface processes in the Earth's lithosphere and upper mantle (such as propagating lithospheric cracks, diffuse extension in the interior of tectonic plates and small-scale sublithospheric convection) can result in similar style intra-plate volcanic features[22,65] led some to question the existence of deep mantle plumes at all[55,56,66,67]. However, advances in seismic tomography have now allowed deep mantle plumes to be imaged with more confidence. Several global-scale mantle tomography studies have shown the existence of broader continuous low-velocity seismic anomalies extending from the deep mantle that can be interpreted as mantle plumes[68–72]. In particular, the first whole-mantle conduit has now been imaged[73] that is sufficiently narrow to be considered a purely thermal plume, as originally proposed[1].

As well as seismic imaging and geodynamic simulations, advances in high-precision geochemical techniques have caused a revolution in understanding the complex formation history of mantle plumes. Most notably, plume-fed hotspots exhibit geochemical heterogeneity, indicating that both ancient domains and recycled crust reservoirs are feeding upwelling plumes, providing insight into mantle dynamics[5,7,74,75]. In some cases, these heterogeneities are expressed on Earth's surface and sustained in bilaterally zoned 'striped' volcanic chains, as seen in Hawaii, Galápagos, Marquesas and other volcanic islands chains[76–82]. In addition, extinct short-lived isotope systems (such as ^{129}I-^{129}Xe, ^{182}Hf-^{182}W and ^{146}Sm-^{142}Nd) indicate the presence of early-formed isotopic anomalies in the source regions of mantle plumes that have remained unchanged since they formed during Earth's accretion from ~4.567 billion years ago until the end of the Hadean[83–85]. These isotope systems also reveal that mantle plumes might even tap into Earth's core[86,87], which was previously considered to be an isolated reservoir not interacting with the mantle.

In this Review, we discuss progress in imaging the lower mantle, in understanding whether low-velocity anomalies are seismic signatures of active upwellings and in modelling the shapes and behaviours of plumes depending on composition and rheology. We confer on how the geochemistry of oceanic island basalts increases knowledge of deep mantle reservoirs and plume formation at the core–mantle boundary. We also synthesize

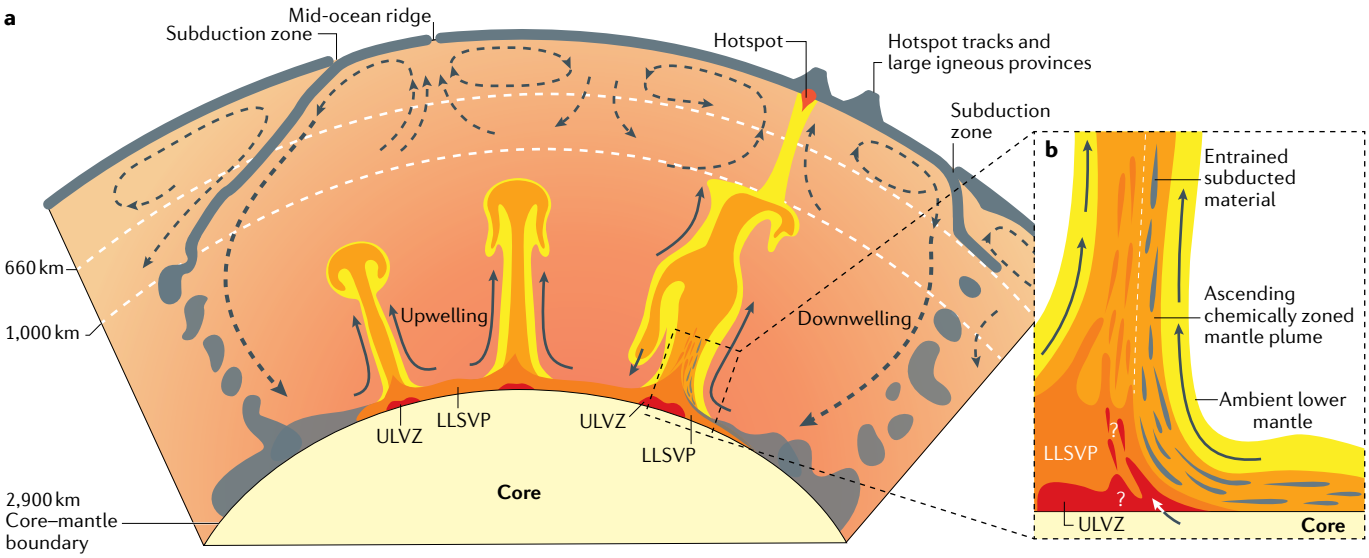

Fig. 1 | **Dynamic nature of Earth's interior. a** | Schematic cross section through Earth's interior, depicting the key components of plume generation and upwelling near, above and along the edges of a large low-shear-velocity province (LLSVP) and near the core–mantle boundary. These LLSVPs might contain localized ultra-low velocity zones (ULVZs) and along their edges subducted material may pile up over hundreds of millions of years. **b** | Schematic cross section of a plume root showing the entrainment of subducted materials, LLSVP and ULVZ components, and possibly core materials at the edge of a LLSVP and centred above an ULVZ (that might be a unique deep mantle locality containing partial melt).

palaeomagnetic and age information in seamount trails in the context of informing past plate and plume motions, including how and if true polar wander might happen, given the observed overall mantle structure. We discuss how continental break-up and the formation of new ocean basins can be affected when mantle plumes impinge on the base of Earth's lithosphere. In addition, we provide a catalogue of more than 50 identified hotspots (Supplementary Table 1), of which 18 are considered most likely to have a deep mantle plume origin. Lastly, we provide perspectives on future integrative research themes that can help improve understanding of mantle plumes and their role in the interconnected Earth system and processes.

Deep mantle superstructures

Based on today's global seismic tomography models, two large-scale features with anomalously low seismic velocities can be recognized in the deepest parts of the mantle (FIG. 2). Although their general outlines and locations underneath the Pacific and below Africa have been known for decades, the composition, fine-scale structure and origin of LLSVPs are still debated, as well as their role in the generation of deep mantle plumes.

LLSVP structure and origin. The first tomographic images of the Earth's lower mantle revealed the presence of a very long wavelength structure at the base of the mantle that is anti-correlated with the gravity field[88]. The first possible explanation proposed was a dynamic interpretation encompassing thermal anomalies and core–mantle boundary deflections owing to mantle-wide convection, and the second involved lateral variations in composition because of the presence of denser eclogite-like material in regions of past subduction and/or chemical plumes originating near the core–mantle boundary. Both the thermal and compositional explanations were quite speculative at the time; however, they are still actively pursued. The large-scale correlation of seismic structure in the deep mantle with anomalies in Earth's geoid and subduction zone configuration[36,89] was established soon thereafter. The correlation with the distribution of hotspots and superswells in oceanic lithosphere was also noticed early on[90–96] and, today, we understand these show a strong correspondence with LLSVP locations (FIG. 2a).

Since then, scores of seismic studies have confirmed the presence of LLSVPs and interpreted the seismically fast areas elsewhere as the remnants of the downgoing slabs from present and past subduction zones[31–33,97] with a time-depth progressive correlation demonstrated for the last 130 million years[35]. Tomographic models show considerable agreement on the extent of the LLSVPs and the shape of their borders on large scales, when filtered up to 2,500-km wavelengths[98–100]. The LLSVP structures are likely hot; however, the anti-correlation of bulk-sound and shear velocities within them[40,42,101,102], as well as the sharpness of their borders[103–105], suggest that they might include a denser component of different composition. In spite of these observations, some studies question the necessity of the denser component[106,107] and imply that LLSVPs could be purely thermal features.

If, indeed, LLSVPs are denser than the surrounding lower mantle[108,109], this would help resist entrainment of LLSVP components in mantle convection and prevent mixing with the overlying mantle. This could help facilitate the survival of LLSVPs over hundreds of millions of years[34] and, perhaps, throughout most of Earth history[110,111]. However, resolving the internal density structure in LLSVPs is challenging[112–114] and different

True polar wander
Reorientation of the entire solid Earth with respect to the spin axis.

Eclogite
An ultra-high pressure metamorphic rock forming at depths greater than 35 km and typically associated with the transformation of basalt during oceanic plate subduction.

Geoid
Equipotential surface of the Earth's gravity field that most closely coincides with mean sea level.

Superswells
Regions of elevated topography too large to be attributed to a single hotspot. Two prominent superswells overlie the corresponding large low-shear-velocity provinces in the Pacific and Africa.

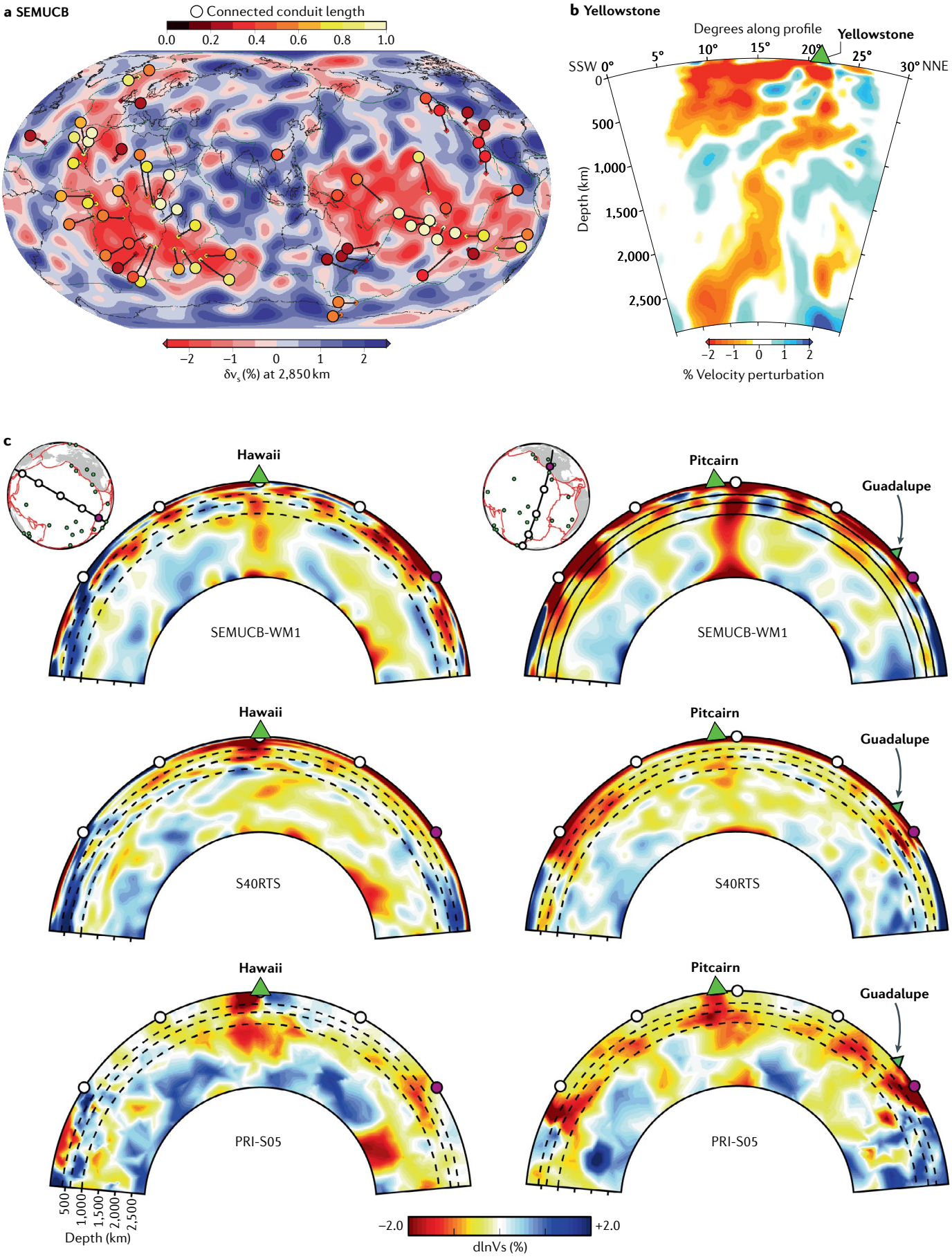
a SEMUCB
Connected conduit length
0.0 0.2 0.4 0.6 0.8 1.0
−2 −1 0 1 2
δv_s (%) at 2,850 km
b Yellowstone
Degrees along profile
Yellowstone
SSW 0° 5° 10° 15° 20° 25° 30° NNE
0
500
1,000
1,500
2,000
2,500
Depth (km)
−2 −1 0 1 2
% Velocity perturbation
c
Hawaii
Pitcairn
Guadalupe
SEMUCB-WM1
S40RTS
PRI-S05
500
1,000
1,500
2,000
2,500
Depth (km)
−2.0
+2.0
dlnVs (%)

Fig. 2 | **Tomographic imaging of mantle plumes and LLSVPs. a** | Global map linking surface hotspots (circles) with depth-projected source locations (diamonds) of the mantle plumes based on the methods of REF.[9], using the plume catalogue of REF.[195] and tomographic model SEMUCB-WM1 (REFS[72,327]). The blue to red background colouring depicts the amplitude of the seismic shear velocity anomaly δv_s at 2,850-km depth in SEMUCB-WM1. Two large low-shear-velocity provinces (LLSVPs; red background colours) are located beneath Africa and the mid-Pacific. Most plumes originate above these LLSVPs with a smaller group (Bowie, Cobb, Guadalupe and Socorro in the eastern Pacific) forming away from these lower mantle anomalous regions. The upper colour bar represents the normalized length of the mantle plume conduits as identified in tomography, where unity (light colours) mean that 100% of the plume length is mapped over the full mantle depth and zero (dark colours) mean that none of the plume length is mapped. **b** | Whole-mantle depth cross section (from the equator about 6° west of Baja California up to 30° N in Saskatchewan, Canada) showing the Yellowstone mantle plume structure (red-orange colours) based on shear wave tomography models using the dense USArray seismic network[73]. **c** | Collage of mantle plume tomography images for Hawaii and Pitcairn that compare three seismic shear wave tomography models developed over the last 15 years: PRI-S05 from REF.[68], S40RTS from REF.[41] and SEMUCB-WM1 from REF.[327]. Small globes show the position of the cross section lines. Panel **b** adapted from REF.[73], Springer Nature.

inferences on their estimated density[115,116] might be because of thermal effects counteracting intrinsic density contrasts to a different extent and in different parts of the LLSVPs[117]. The distinct composition and observed chemical heterogeneity of the two LLSVPs could result from a reservoir of primitive material at the base of the mantle, as suggested by the relationships between high $^3He/^4He$ hotspots and plumes originating near the core–mantle boundary[87,118–121], from the accumulation of subducted crust transformed into eclogite[34] or from some depth-dependent stratification of both[111]. However, whether the LLSVPs are compact, continuous piles of compositionally distinct material[11,43,122] where mantle plumes are generated across their tops and along their edges or whether LLSVPs represent bundles of closely spaced thermochemical plumes[64,123] separated by a ring of downwellings that are constrained by the geometry of tectonic plates at the surface[124,125] remains a subject of debate[37,117,123,126].

Mantle plume nurseries. Also debated is whether or not plumes — specifically, those that can be correlated to ancient LIPs — originate primarily along the edges or anywhere above LLSVPs[8–15]. LLSVP edges are defined by sharp vertical and horizontal gradients in seismic shear-wave velocities[103,105,127]. Many plumes and reconstructed LIP locations tend to occur close to vertically above LLSVPs (FIG. 2a). Hence, LLSVPs are proposed by some to act as plume generation zones or nurseries for all major deep-mantle-sourced hotspots and LIPs that have been active and remained approximately in place over at least the last 200 million years[110,128–130]. However, because the African LLSVP is rather narrow (FIG. 2a), a concentration of plumes near the edges is ambiguous. Interestingly, the roots of at least some of the LLSVP-rooted plumes do seem to contain unusually large ultra-low velocity zones (ULVZs). For example, mantle anomalies below Hawaii[131], Samoa[132], Iceland[133] and Marquesas[134] are indicative of a compositionally different, likely denser, component[117,135], possibly because of the presence of partial melt[136] or at least iron enrichment[137,138] in these ULVZs.

Ultra-low velocity zones
(ULVZs). Smaller regions (hundreds of kilometres in size) of very low shear velocity (exceeding 10% lower than average) in the lowermost few tens of kilometres of the mantle. There are perhaps a dozen or more of them.

Thermal mantle plumes
Columnar upwellings of hot material from the lowermost mantle to the base of the lithosphere.

Hotspot swells
Regions of elevated topography (several hundred kilometres wide) caused by buoyant mantle plume material rising beneath and being dragged along with a moving plate.

Thermochemical mantle plumes
Columnar upwellings of hot and chemically distinct material from the lowermost mantle to the base of the lithosphere.

Mantle plume characteristics

In this section, we discuss what geodynamic modelling predicts about the make-up and behaviour of plume heads and tails during plume generation and ascent, and we review what seismic imaging reveals about deep mantle plumes.

Models of plume generation and ascent. Localized hot upwelling plumes are expected in any terrestrial-type planet mantle, where convection operates through bottom heating in a temperature-dependent viscosity fluid of uniform composition or where a domain with concentrated heat production can sustain a thermal boundary layer[25,26,59,139,140]. Differences in temperature and/or composition will cause variations in density that can result in thermochemical instabilities near boundary layers as the beginning of an upwelling and, when it persists, a rising mantle plume[25].

Typical thermal mantle plumes in Earth are expected to have a broad plume head, up to roughly thousand kilometres in diameter, followed by a narrow plume tail, not wider than a couple of hundred kilometres[23,28,57,141,142]. These plumes can persist over long geological times, but only if the thermal boundary layer from which they arise is also maintained for hundreds of millions of years. Indeed, for plumes to keep rising through the entire mantle, a lower limit of ~500–1,000 kg s^{-1} of anomalous mass flux (volume flux times density anomaly) is required to sustain the plume tails[143]. Anomalous mass flux can be estimated from the size of hotspot swells[21,57,90,144,145], the interaction of plumes with migrating spreading ridges[146,147], the geometry of V-shaped ridges[148] or based on seismic tomography[149]. However, owing to different amounts of buoyant material available in the thermal boundary layer, the anomalous mass flux is expected to vary between plumes and can change with time for individual plumes[144,145].

Even though rising plumes from near LLSVPs are expected to be buoyant owing to their hotter temperatures, they are also likely to entrain chemically distinct materials from the LLSVPs that can be denser than the surrounding mantle[115] and, thus, their positive buoyancies might be substantially reduced[34,150]. The anomalous density of LLSVPs[115,116] and the nature of the entrainment of other materials during ascent of these thermochemical mantle plumes[151,152] are still debated. Because of time-dependent and variable amounts of entrainment, highly complex plume behaviour and shapes (FIG. 3) can result that substantially differ from the classical head-and-tail structure[153–155]. For example, the negative buoyancy of material entrained from LLSVPs in plume heads can cause material to sink back into the ascending plume[156,157], leading to broader plume conduits that are a few hundred kilometres wider than typical thermal plumes.

How long it takes for a plume head to traverse the mantle after forming at the core–mantle boundary is difficult to estimate. It primarily depends on its buoyancy, arising from a density contrast of ~30 kg m^{-3} for thermal plumes, but which could be much less for thermochemical plumes, and the average viscosity of the surrounding mantle. Widely discrepant estimates exist for

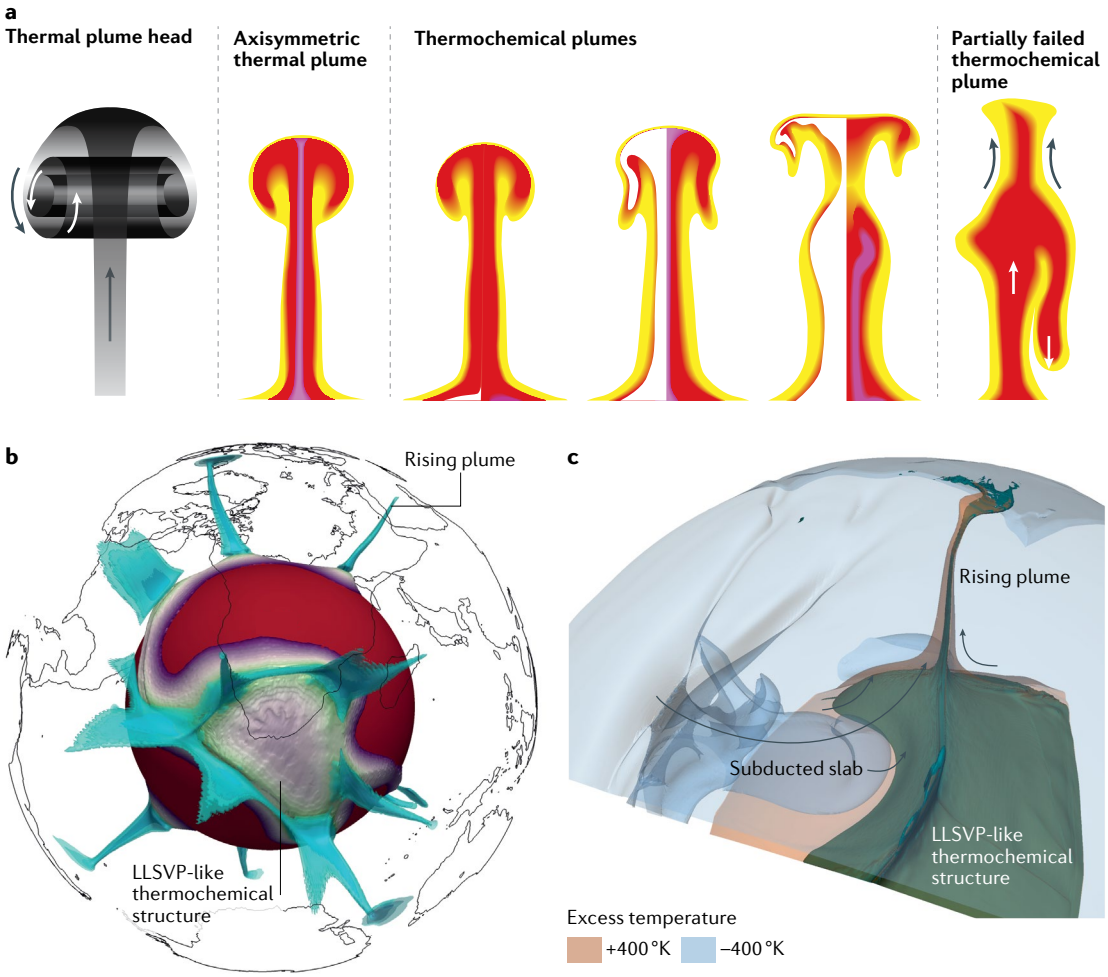

Fig. 3 | **Examples of rising thermal and thermochemical plumes. a** | Representations of rising thermal plume head models: a thermal plume head connected by a stem to the source region[27]; an axisymmetric thermal plume; three thermochemical plumes[150] with colours representing temperature differences (purple/red = hottest; orange = cooler; yellow = coolest; white = chemically different plume material); and, finally, a model of a plume that partially fails when entrained materials (that are too heavy) collapse in the top of the conduit (based on laboratory syrup tank experiments[155]). **b** | 3D and time-dependent numerical model with plumes (blue) rising from a large low-shear-velocity province (LLSVP) situated below southern Africa[13]. **c** | 3D model showing rising plumes from the LLSVP margins that are substantially hotter than the surrounding lowermost mantle, with large temperature anomalies of about 500 K (REF.[77]). Panel **b** adapted with permission from REF.[13], Wiley, © 2015. American Geophysical Union. All Rights Reserved. Panel **c** adapted with permission from REF.[77], Proceedings of the National Academy of Sciences.

mantle viscosity, as it can be (locally) controlled by variations in temperature and stress that might render global average viscosity estimates not applicable for plumes[158]. One traversal time estimate can be made because reconstructed LIP eruptions are correlated with LLSVP margins and, therefore, LIPs are hypothesized to erupt from those margins[129,159]. However, in order for that correlation to be maintained during their rise through the mantle, plume heads must rise up from the lower mantle rather fast, probably within 30 million years or less, to avoid large lateral deflections, consistent with numerical models[13]. For smaller plumes with smaller plume heads, such as the Yellowstone plume (FIG. 2b), the plume heads are predicted to rise more slowly, taking 80 million years or longer[160]. Despite these long ascent times, plume heads rise considerably faster than slabs sink, which are estimated to sink at speeds of 1–2 cm per year, such that slabs require between ~150 and 200 million years to reach the bottom of the mantle[13,31,161,162].

As plumes rise through the mantle, they are predicted to become increasingly tilted with time as their roots become shifted towards large-scale upwellings, likely above the two LLSVPs[62,163]. Numerical models yield tilts (mostly) up to — but sometimes even exceeding — 60° (REFS[11,62,164]). These strong tilts are partly a consequence of plumes being modelled such that they match the present-day hotspot positions; the tilts tend to be less in models where plumes dynamically form, but do not exactly match actual hotspot positions[11,13,77,165]. Eventually, when the plume head reaches the lithosphere, a LIP can form over short amounts of geological time, likely in less than a million years[108]. Long-lived hotspot tracks can form after that and persist in some cases for 80 to 120 million years[60,166,167] or even longer[79].

Several hotspot tracks are associated with flood basalts at one end (such as Tristan, Réunion, Kerguelen) and, thus, might correspond to typical thermal plumes with a tail following a plume head[28,168].

Although the typical lifetime of a deep mantle plume is likely long, on the order of ~100 million years, some of the older Pacific oceanic plateaux (for example, Hess and Shatsky Rise) were volcanically active only in the Cretaceous and do not correspond to any currently active hotspot[169,170]. Evidence from the bathymetric record in the Pacific Ocean also indicates that many hotspot trails are characterized by shorter seamount trails, apparently only active for up to 30 million years[171,172]. These surface expressions, however, do not have to mean that the mantle sources are short-lived per se but, rather, that instabilities can develop in rising mantle plumes, for example, once conduits are tilted more than 60° from the vertical, they might break apart[163,173]. Other studies suggest that plume heads might cut themselves off from a supply of hot mantle material[153] or detach from their plume conduit[174]. Plumes might also become internally unstable and collapse (FIG. 3a) because of their insufficient buoyancy[155] or else switch on or off if rising plumes are pulsating or boudinaging[150,154].

All possible explanations for such intermittent plume behaviours and plumes without heads are still being mapped out and debated. Some hotspot tracks end at subduction zones and it has been proposed that the respective LIP might have been accreted to the overriding plate, for example, for the Hawaii plume in Kamchatka and the Okhotsk Sea[175]. An alternative hypothesis is that the Hawaiian flood basalts might have been subducted into the upper mantle below Kamchatka[176].

Imaging mantle plumes. Within the framework of purely thermal convection, thermal mantle plume conduits are expected to be only 100–200 km in diameter in the upper mantle and no more than 400 km in the lower half of the mantle, which has a higher viscosity by about two orders of magnitude[177]. Given these predicted small plume conduit diameters, plume detection via seismic tomography is especially difficult, because of limited resolution owing to a lack of earthquake sources and receiver stations in the ocean basins[58,178–180]. In addition, plume signals might be hiding in the small-amplitude coda of shear and compressional seismic waves, so that the full waveforms must be analysed in their entirety to better resolve plume conduits, as illustrated by synthetic experiments[181]. Such new analytical approaches, therefore, are required to resolve the smaller wave speed variations that could be interpreted as plume-like conduits in seismic tomography.

In earlier studies, teleseismic travel time tomography has found plume-like conduits of at least 400 km in diameter[182–184]. For example, the Iceland plume at first could only be seen in the upper mantle with an upwelling broader than expected[185,186], and imaging of the Hawaii plume originally resulted in the detection of a broad, inclined upwelling, disappearing from view below 1,500-km mantle depths[68,187,188]. However, in higher-resolution models, broader (>400 km) plume-like conduits are found beneath many major hotspots, and they appear to be rooted near the core–mantle boundary and extend into upper mantle depths in the vicinity of hotspots[69,71,72] (FIG. 2c). Numerical models show that thermochemical plume conduits are wider than a purely thermal plume[156], in order to attain sufficient buoyancy. Hence, plume conduits larger than ~500 km in diameter as observed in tomographic models indicate that they are likely thermochemical rather than purely thermal[72,189], and most of these broad conduits are observed over the LLSVPs (FIG. 2a). Anomalies in the travel times of seismic core waves, recorded by the dense USArray seismic network in North America, now also reveal a low-velocity plume-like anomaly in the lower mantle beneath the Yellowstone hotspot[73] (FIG. 2b) that is probably unrelated to the Pacific LLSVP.

These seismically imaged, low-velocity plume-like structures are nearly vertical in much of the lower mantle, but some are strongly tilted above a depth of 1,000 km (REF.[72]), which is different from geodynamically modelled conduits that tend to be tilted throughout the entire mantle[62,177]. Such a strong tilt above ~1,000 km is also found for the Yellowstone plume[73], which, so far, is the only plume where the predicted tilted conduit shape can be matched in detail with a tomographic conduit image[160]. The difference in tilt from geodynamic modelling and seismic observations can provide important constraints on mantle rheology. It might indicate that the overall large-scale mantle flow at depths greater than ~1,000 km could be substantially slower than currently modelled, with horizontal flow speeds not exceeding a few millimetres per year.

In addition, global seismic tomography indicates that both downgoing slabs[190] and broad upwelling plume conduits[69,72] appear to be deflected horizontally around a depth of 1,000 km. This deflection is deeper than the known deflection at 660-km depth — where there is a seismic discontinuity that most likely corresponds to a phase transition from less dense ringwoodite crystal structures to denser lower mantle bridgmanite and other high-pressure oxides — and is accompanied by a decorrelation between the longest wavelength seismic structures in the extended transition zone (400–1,000 km) and the deeper mantle[191]. Similar observations were already visible in lower-resolution seismic mantle models and indicated by seismic data suggesting a vertical decorrelation at ~800-km depth[192]. The 1,000-km boundary, thus, may require a change of material properties not coinciding with the 660-km discontinuity and could be explained by an increase in mantle viscosity somewhat deeper than traditionally considered, given the rather non-unique constraints provided by geoid and post-glacial rebound data[193,194].

In summary, there is still progress to be made in resolving ~100-km-scale seismic heterogeneities in the lower mantle relevant to the scale of deep mantle plumes. However, modern-day global tomography models are starting to resolve the presence of deep mantle plume conduits below hotspots.

Deep mantle plume catalogue. We compiled a deep mantle plume catalogue (Supplementary Table 1) based on a listing of 57 potential hotspots[195] that was then

Ocean island basalts
A volcanic rock type typically of basaltic composition, forming in ocean basins away from plate tectonic boundaries and associated with intra-plate hotspot volcanoes and mantle plumes.

individually scored by the authors of this paper in order to generate an expert opinion poll average, with the aim of providing a database of hotspots ordered by strongest to weakest evidence for a deep mantle plume origin. In their scoring, each of the authors used their own set of criteria, but everyone could score plumes of deep origin as probably (1 point), perhaps (0.5 points), not (0 points) or unknown (no score). We added up all points and divided these by the number of scores given for each plume. The full catalogue (Supplementary Table 1) and a map (Supplementary Figure 1) lists only 18 plumes above the threshold of 0.8 points that are most likely to have a deep mantle origin. These high scores in our plume rankings suggest strong evidence for a deep mantle plume beneath a hotspot; however, the reader should be careful when interpreting lower scores to mean that we exclude the possibility of a plume. Because we have not yet observed a plume beneath a hotspot does not mean that such a plume does not exist, owing to imperfect seismic datasets and models or missing ages and/or geochemistry data.

One concern is that Yellowstone-type plumes might exist beneath hotspots with lower scores in the table, in particular, for the African continent, as we understand now that such plumes are 'thin plumes' that are observed only when datasets from high-density seismic arrays are available[73]. Another concern is that high $^{3}He/^{4}He$ can be indicative of a deep mantle conduit sourcing a hotspot, but the lack of high $^{3}He/^{4}He$ does not exclude the presence of a plume, as many plume-fed hotspot volcanoes only exhibit low helium isotope ratios[196]. In addition, a short hotspot track does not exclude a plume, because the plume could have arrived in the shallow mantle only over the last few tens of million years[197] or the hotspot could have exhibited only intermittent volcanic activity over the last ~140 million years[171]. Finally, hotspots that are so closely spaced that they correspond to separate upwellings in the upper mantle, but likely one (wider) upwelling in the deep mantle, are considered as one hotspot. Examples are Tristan-Gough and Bouvet-Meteor/Shona.

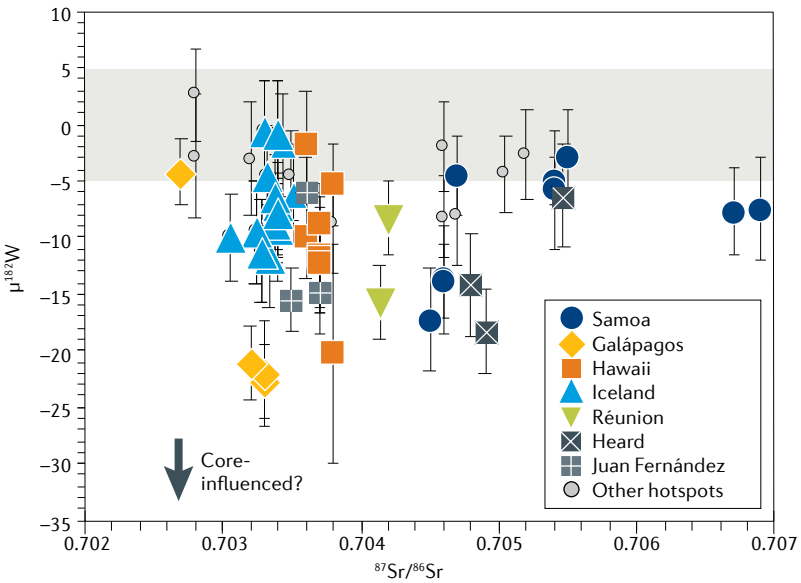

Fig. 4 | **Isotope systematics in global plume volcanics.** Negative $\mu^{182}W$ anomalies appear in some plume-generated ocean island basalt volcanoes, with no relation to long-lived $^{87}Sr/^{86}Sr$ signatures, but a relation between $\mu^{182}W$ and the presence of recycled oceanic and continental material does emerge from the data[239]. One interpretation of these observations is that some deeply sourced mantle plumes with strongly negative $\mu^{182}W$ anomalies have inherited a W-isotopic signature of Earth's core[86,87], but other interpretations exist, as discussed in the main text. The grey band represents the 2σ reproducibility (±5 ppm) on the terrestrial tungsten isotope standard, which, by definition, has $\mu^{182}W = 0$. Data and errors shown are 2σ measurement errors summarized in REFS[87,239]. We note that the estimated $\mu^{182}W$ is as low as −220 in Earth's core[328].

Geochemical heterogeneity

Although hotspot trails and LIPs have complex histories, variations in their chemical compositions provide clues about the number and nature of distinct domains that reside in Earth's interior and that are sampled by mantle plumes. These clues lead to intriguing debates on where and at what length scales and timescales those geochemical domains are manifested in the deep mantle, and how geochemically and geographically zoned hotspot trails might reflect heterogeneity within mantle plumes.

Enduring ancient signatures. Extinct short-lived isotope systems provide insights into the processes happening in the earliest approximately 50 (for ^{182}W) to ~500 million years (for ^{142}Nd) of Earth's history[85,120,198,199]. Because radioactive decay in these isotope systems is rapid, with half-lives from 8.9 to 103 million years, the radioactive parent isotopes were only present in the early stages of the Earth's formation, so resolvable changes in the radiogenic isotopic ratios of $^{129}Xe/^{130}Xe$, $^{182}W/^{184}W$ and $^{142}Nd/^{144}Nd$ are restricted to the Hadean, which ended 4 billion years ago. The presence of such ancient isotopic anomalies in mantle plume source regions, therefore, suggests that some early-formed mantle reservoirs are still present in the Earth's interior, despite extensive convective mixing[83,84,87,119]. For example, the ^{129}I-^{129}Xe system shows a marked difference in $^{129}Xe/^{130}Xe$ between Earth's mantle and atmosphere[29] indicating that heterogeneous $^{129}Xe/^{130}Xe$ signatures are preserved in the mantle since the Hadean[83]. Datasets for the ^{182}Hf-^{182}W and ^{146}Sm-^{142}Nd systems confirm the presence of Hadean-generated signatures in the modern mantle, with resolvable ^{182}W (FIG. 4) and ^{142}Nd anomalies in plume-fed ocean island basalts[84,120,200], but the discovery of anomalous ^{182}W in plume-head-generated flood basalts[86] remains controversial[201].

Several studies found that most ocean island basalts that host negative ^{182}W anomalies also exhibit high $^{3}He/^{4}He$ lavas[87,120,121] that, in turn, could be interpreted to sample deep primordial mantle signatures[202] present in only the hottest and most buoyant (deep) mantle plumes[196]. It is hypothesized that these ocean island basalt ^{182}W anomalies reflect a contribution from Earth's core, which has preserved a very low $\mu^{182}W$ value (the deviation of $^{182}W/^{184}W$ from the terrestrial standard in ppm). This extreme core value developed because tungsten is a moderately siderophile element that, during core formation, became enriched in the Earth's core relative to the short-lived, lithophile radioactive parent (^{182}Hf) that remained in the mantle[86,87]. It is possible that this core material is partitioned back into the mantle at

the base of mantle plumes, aided by silicate melting[87] and possibly in ULVZs at the core–mantle boundary (FIG. 1b). However, the origin of the low $\mu^{182}W$ values as observed in the mantle sources of ocean island basalts can be attributed to late accretion[203] or early Hadean silicate Earth differentiation[204], and it will be important to further evaluate which models are consistent with the positive $\mu^{182}W$ and $^{3}He/^{4}He$ correlation in hotspot lavas[87].

Mantle plume heterogeneities inferred from hotspots. In addition to sampling ancient reservoirs in the deep Earth, mantle plumes erupt lavas that exhibit geochemical signatures associated with several different ancient subducted crustal materials. These surficial geochemical signatures in mantle plume source regions, therefore, provide first-order evidence that Earth is recycling its lithospheric plates in subduction zones at a global scale and is resupplying the deep source regions of mantle plumes with various crustal materials[205–210]. Radiogenic isotopes (such as $^{87}Sr/^{86}Sr$, $^{143}Nd/^{144}Nd$, $^{206}Pb/^{204}Pb$ and $^{176}Hf/^{177}Hf$) provide insight into which, how many and in what way different recycled materials are involved in the chemical dynamics of mantle plume formation[5–7,45,47,74,75], and show that many of the global hotspot systems have two, three or more distinct components in their mantle plume source regions[76,79,82,211–213].

Oceanic and continental crust, and associated sediments, have long been thought to contribute to much of the mantle's compositional variability sampled by plumes[5–7,214–217]. Recycled marine carbonate[218], recycled metasomatized oceanic or continental mantle lithosphere[219–222] and processes occurring at the core–mantle boundary[223] are among the proposed mechanisms for the generation of compositional variability in the mantle and, consequently, in providing the building blocks of (deep) mantle plumes. However, the hypothesis that ancient subducted oceanic crust is returned to the surface in upwelling plumes was challenged because subducted crust can appear too dense, and, instead, it has been postulated that upper mantle peridotite is the predominant lithology melting beneath plume-fed hotspots[110]. However, other studies show that recycled mafic (eclogite and pyroxenite) lithologies (derived from subducted oceanic crust) are, ultimately, needed in generating the major element compositions of ocean island basalts[224–226]. Recycling of materials that were once at the Earth's surface and from as early as the Archaean[207,227,228] therefore appear to be required to explain the geochemical variability in plume-fed hotspot lavas.

Primordial and recycled reservoirs inferred from plume-fed hotspots. Mechanisms for the long-term preservation of the Hadean geochemical anomalies are imperfectly understood[229], but storage in dense, viscous domains of the deep mantle can isolate Hadean-formed reservoirs from convective motions of the mantle[146,150,230]. The two LLSVP regions at the core–mantle boundary are attractive locations in this regard[83,118] and plume-fed hotspots may provide important clues. For example, hotspots with the highest (most primordial) $^{3}He/^{4}He$ ratios appear to be positioned over the LLSVPs[118,119]. This appears consistent with an ancient source for these seismic features, though the high $^{3}He/^{4}He$ Yellowstone hotspot[231] that is positioned outside of the LLSVP regions[73,160] suggests that primordial domains might also exist outside of the LLSVPs[195]. However, to date, ^{129}Xe, ^{142}Nd and ^{182}W short-lived isotope datasets in ocean island basalts are still statistically too small (FIG. 4) to conclusively link the Hadean isotopic anomalies to the LLSVPs. Much larger Sr–Nd–Pb isotope datasets confirm that hotspots with geochemically enriched (low) $^{143}Nd/^{144}Nd$ are geographically linked to both of the LLSVPs[82,232,233]. These enriched mantle domains are concentrated in the Southern Hemisphere[234] and appear to exist at the largest (hemispheric) length scale in the mantle[46], although geochemical heterogeneities also exist at much shorter centimetre to kilometre length scales[235] or even sub-centimetre scales in peridotite samples[236]. Some have suggested that only the African LLSVP hosts these enriched (low) $^{143}Nd/^{144}Nd$ mantle signatures[237], but such arguments hinge on the selection of plumes[195] and more work is needed to better identify reservoir geometries and dynamics. Global hotspots with higher radiogenic Pb isotopes (with increased $^{206}Pb/^{204}Pb$) seemingly are not linked to the LLSVPs[75] and, thus, leave the location of this scarce mantle domain uncertain. Finally, it has been argued that neither recycled oceanic crust nor continental crust are specifically associated with the LLSVPs[119] and that hotspots with low $^{143}Nd/^{144}Nd$ signatures and hotspots with radiogenic Pb isotopic signatures appear to be spatially decoupled in Earth's mantle[195]. This decoupling is unexpected, given that both mantle domains are likely to have formed via subduction and recycling as part of the plate tectonic cycle.

ULVZs are argued to be compositionally distinct from their surrounding mantle and from LLSVPs when they are hosted within those dense layers[238]. Thus far, only a few plume conduits, including Hawaii, Samoa, Iceland and Marquesas, can be associated with ULVZs[131–134]. However, it is not yet possible to evaluate whether ULVZs sample geochemical mantle reservoirs that are different from LLSVPs. Until the ULVZs have been conclusively mapped out in seismic images, it will not be possible to determine whether ULVZ-related plumes have a different composition than plumes that are not related to ULVZs, and this currently limits what can be inferred about the isotope geochemistry of the ULVZs. Ultimately, the evolution of these geochemical domains is linked to plate tectonic processes, including recycling of oceanic and continental crust and transport by plumes, and these processes control the composition, location, size, amount of chemical overprinting[239] and longevity of geochemical reservoirs in the Earth's interior.

Chemical plume structures. Surface expressions of plume-fed volcanism in the oceanic realm are highly varied. A notable complexity is the formation of double-track volcanic hotspot trails that exhibit a bilateral geochemical zoning or striping over millions of years of plume history. These kinds of surface expressions can be governed by the make-up of the plumes themselves[76–82] and by their interactions with the overriding tectonic plates and any changes in plate motion

Peridotite
The dominant mantle rock type mostly made from silicate minerals olivine and pyroxene, rich in Mg and Fe, with less than 45% silica.

and direction[240,241]. The presence of these geochemically resolved dual volcanic trends in ocean island systems was first noticed for the Hawaiian Islands[242] and follow the subparallel Loa and Kea volcanic tracks[243] (FIG. 5). Since then, these double-track trends have been observed in many other hotspot tracks, including Cape Verde, Easter, Galápagos, Marquesas, Samoa, Society, Tristan-Gough and Rurutu[79,81,212,244–250].

There are currently several models on the origin of the chemical structure of mantle plumes and the role that this structure plays in generating the observed double-track hotspot trends. The primary models (FIG. 5) invoke different mantle components in an unzoned heterogeneous plume[22,241,251], a concentrically zoned plume[241,252–255] or a bilaterally zoned plume[76–79,81,82,246]. The unzoned heterogeneous plume model calls for plumes with different mantle components that are evenly distributed or contain no notable internal organization[241,251,256]. These models typically rely on variations in both the temperature profile in the plume conduit and melting rates, and differences in the refractory nature of various elements to explain geographic variations in isotopic compositions[251,256] or the generation of small-scale sublithospheric cells[22]. Melting of peridotite and pyroxenite lithologies at differential depths in a tilted plume conduit[241] could then lead to the emergence of double-track volcanism, but this is dependent on a change in the direction of the overriding tectonic plate.

When plume tilt and plate motion are aligned — for example, as hypothesized for the Northwest Hawaiian Ridge — then both melt sources overlie each other, and no zonation is observed. When a change in plate motion would occur — such as the proposed shift in Pacific Plate motion ~6 million years ago — the lithospheric motion could become faster than plume tilt can adjust for, resulting in a geographic separation of deeply sourced peridotite melts (Kea composition) and shallower secondary pyroxenite melts formed from eclogitic melt reactions

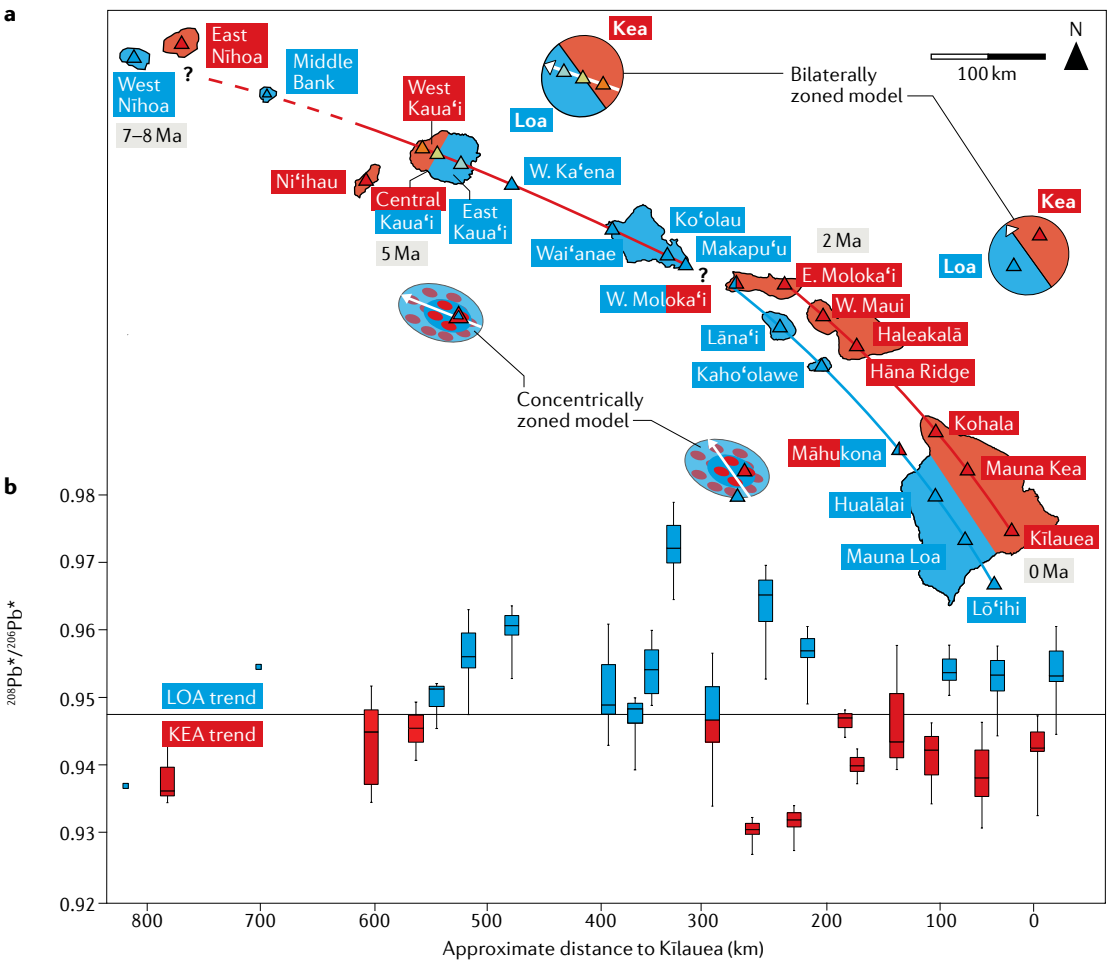

Fig. 5 | **Isotopic zonation of the Hawaiian plume.** Double-track volcanism present among the Hawaiian Islands as evident in Pb-isotopic ratios for lava flows as a function of distance from the active underwater Lō‘ihi volcano[264]. **a** | The location of the Loa (blue) and Kea (red) isotopic trends are superimposed on a map of the Hawaiian Islands with its major active and inactive volcanic centres (triangles). **b** | The box-and-whisker plots of $^{208}Pb^*/^{206}Pb^*$ provide a direct measure of the difference in $^{208}Pb/^{204}Pb$ and $^{206}Pb/^{204}Pb$ as measured in the Hawaiian lavas relative to the composition of chondritic meteorites that formed our Solar System ~4.6 billion years ago. The $^{208}Pb^*/^{206}Pb^*$ ratios, therefore, provide insight into the chemical heterogeneity within the Hawaii plume, which, for this isotopic ratio, is the time-integrated function of the Loa and Kea plume source differences in Th/U. Ma, million years ago. Figure adapted with permission from REF.[264], Wiley. © 2019. American Geophysical Union. All Rights Reserved.

(Loa composition). This model infers that double tracks only appear during periods of plate motion change, and, therefore, does not explain the complex zonation patterns observed along, for example, the Tristan-Gough track on the African Plate[79].

The concentrically zoned plume model argues that plumes concentrate the hottest and densest materials in their centres during ascent from the core–mantle boundary[241]. Concentric zonation is mostly seen in the distribution of primitive helium isotopic signatures[253–255]. The origin of this zonation has been hypothesized to result from higher rates of melting in the plume core relative to the surrounding asthenosphere[253,254] or preferential concentration of dense, primitive material near the core of the plume[255,257]. Alternatively, preferential distribution of helium into carbonate melts could result in more primitive, higher $^{3}He/^{4}He$-bearing melts ascending faster (and more vertically) than solid plume material, and, thus, resulting in a geographically zoned pattern of distinct helium signatures on the surface, which are not reflective of the underlying chemical structure of the plume[258].

The bilaterally zoned plume model postulates that the geochemical zonation observed among most ocean island chains originate from a mantle plume structure that is divided into two distinct chemical domains. The plume could contain a bilaterally continuous structure[80], two zones consisting of vertically continuous filaments with some spacing in between[76], or a partly ordered structure with some mixing between the zones[251]. As some mantle plumes appear to be rooted on the boundary between the LLSVPs (and/or ULVZs) and the geochemically depleted ambient lower mantle (FIG. 2), it is possible that zoned plumes sample distinct materials from these LLSVP 'edge' domains in the lowermost mantle[80,81,259,260].

In the case of Hawaii, the southern Loa component would represent incorporation of more enriched LLSVP materials, whereas the northern Kea component would represent ambient (more primordial) lower mantle materials[82] that are common to most Pacific plumes[261]. However, to explain the general (but incomplete[262]) absence of a Loa component in the Hawaiian plume prior to ~5 Ma, it is required that the LLSVP-derived Loa component only became entrained in the plume conduit intermittently between ~47 and 6.5 Ma, and then more consistently from 6.5 Ma to the present day[263]. Alternatively, this shift from Kea-only to dual Loa-Kea components could also have resulted from a change in plate motion around 6 Ma, as the plate traversed over a bilaterally zoned plume[264]. Similar bilateral trends are seen within several other Pacific hotspots[81,246,259], allowing us to link surficial geochemical signatures to the lowermost mantle geophysical domains (such as LLSVPs and ULVZs).

The bilateral zoned plume appears to be the currently favoured model; however, a combination of different models is also feasible. For instance, plumes can contain bilateral zonation of recycled and ambient mantle components, whereas dense primordial components preferentially concentrate in the plume core. With all plume models, the depth and degree of melting — which relate to plume temperature, lithospheric thickness and the lithology that is melting — can alter the resulting lava compositions. In addition, changes in plate motion can strongly influence how different components in the plume are sampled. Therefore, multiple petrological, chemical and physical parameters need to be considered when further refining and testing models of plume structure.

Mantle plumes and plate tectonics

Understanding if and why certain plumes move, in which directions, in unison or not, and how fast is an ongoing debate. In this section, the evidence that plumes can move independently and at speeds typically less than plate tectonic movements are described. We also discuss how plumes provide insights into possible reorientations of the entire Earth relative to its spin axis, during events of true polar wander, and how they are considered powerful initial mechanisms in the global plate tectonic cycle, for example, in breaking up continents or initiating subduction.

Distinguishing plume motions. The presumed stability of thermal mantle plumes initially allowed scientists to use the shapes and age progressions of seamount trails to derive directions and speeds of past plate motions, and, with those models in hand, to chart out the positions of tectonic plates back through geological time[1,2,159,169,265–269]. In these models, fixed mantle plumes were presumed to persist over more than 100 million years. It would be expected that all seamount trails forming on a particular tectonic plate would record the same history of plate motions around the same Euler poles. It would also be expected that, when plate motion changes occurred, the timing of the bends (or turns) that would form in each seamount trail would be contemporaneous (BOX 1). In other words, in a fixed mantle plume scenario, the geometries between different seamount trails would be fixed and their chronologies identical.

Palaeomagnetic inclination data from seamount trails indicate that plumes are, in fact, not stationary with respect to the spin axis[166,270,271]. Distance comparisons between coeval seamount trails show that plumes are moving away from or closing in on each other[60,272], and the $^{40}Ar/^{39}Ar$ dating of the Louisville and Rurutu hotspot tracks on the Pacific Plate show that the most acute parts in their bends (not as pronounced or clearly visible as for Hawaii) appear to occur around 47 Ma and thus about 3 million years earlier than the Hawaiian-Emperor bend[60,248,273,274] that exhibits its strongest bending around 50 Ma. For these Cretaceous and early Cenozoic times, analysis of related palaeomagnetic data and age dates concluded that the Hawaiian hotspot moved at 48 ± 8 mm per year between 63 and 52 Ma, whereas other Pacific hotspots have moved much more slowly[275]. Similarly, based on age progressions along tracks and changing distances between tracks, a total relative motion of 53 ± 21 mm per year between Hawaii and Louisville and of 57 ± 27 mm per year between Hawaii and Rurutu has been found, pointing to a likely large individual Hawaiian hotspot motion from 60 to 48 Ma, compared with more limited plume motions for Louisville and Rurutu[60]. Such observations

Euler poles
Poles describing the rotation of a plate on a sphere. Any rigid plate motion can be described as rotation around an Euler pole.

Box 1 | **Scenarios for Hawaiian–Emperor bend formation**

The prominent 120° bend in the Hawaiian–Emperor seamount trail (HEB; see figure) was first interpreted as representative of a major change in Pacific Plate motion[267] occurring ~47 million years ago (Ma)[274]. However, an absence of geological evidence for a change in Pacific Plate motion at that time, and recognition that hotspots are mobile, led to the proposal that the HEB might represent Hawaiian hotspot motion, which came to an abrupt stop at the time of the bend[329]. This hypothesis was tested through the analyses of magnetic palaeolatitudes in scientific ocean drilling cores recovered from Emperor seamounts, which support a notable southward hotspot motion between ~80 and 47 Ma (REFS[270,275,330]). Comparison of the relative distances of Pacific hotspots using age progressions along three tracks (Hawaii, Louisville and Rurutu) show the Hawaiian hotspot moving southward, with a maximum ~600–700 km of motion occurring between 62 and 47 Ma that is insufficient to explain the entire, more than 2,000 km, length of the Emperor chain[60]. There remains an active debate on the relative contribution of hotspot drift and plate motion changes to the shape of the 120° bend, with scenarios ranging from the HEB being entirely caused by a ~60° change in plate motion[331,332] to being mostly caused by hotspot drift[271,275,276]. In this debate, however, it is becoming apparent that at least one-third of the length of the Emperor chain can only be explained by a southward Hawaii plume motion in the beginning of the Cenozoic.

The three plate reconstructions shown in the figure all use the Antarctic Plate circuit. Two of them (REFS[280,333]) use relative motions in Zealandia as additional constraints, whereas (REF.[334]) does not. The mismatch between the predicted 47-Ma hotspot locations and the actual location of the bend (Daikakuji Seamount) is consistent with ~1 cm per year south-east hotspot motion (short orange arrows) from 47–0 Ma that is obtained by numerical models[276,332]. The mismatch between the predicted 61-Ma hotspot locations and Suiko Guyot can be amended by adding another second rapid southward hotspot motion (long maroon arrow) that is consistent with age progressions along the hotspot tracks[60] and numerical modelling[276].

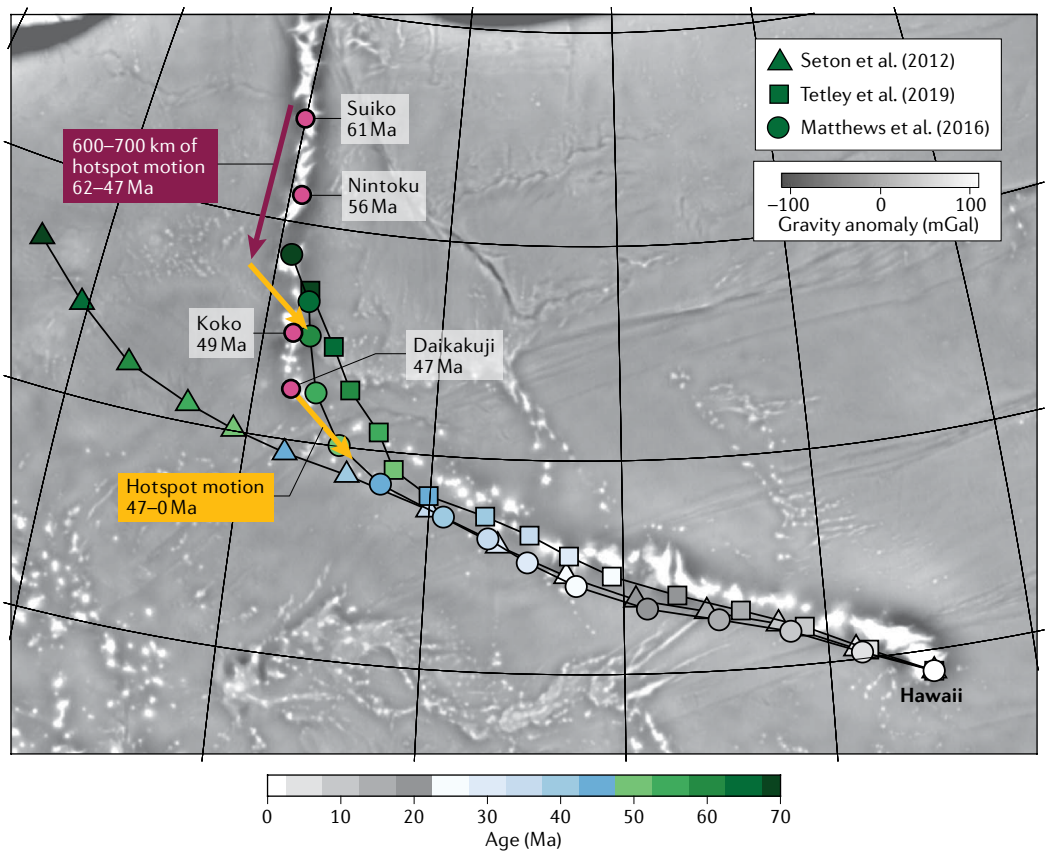

are not unexpected in a convecting mantle, as computer models show that rising mantle plumes will be advected in Earth's overall mantle circulation regime[62,163,276,277] and cause the locations of hotspots on the Earth's surface to wander over geological time.

For the most recent 5 million years in Earth's history, the rate of motion of major hotspots can be computed differently using a maximum likelihood optimization that incorporates present-day plate motion models[278] and which is compared with the azimuths and age progressions of hotspot tracks[279]. This alternative kinematics-based modelling approach obtains hotpot motion rates[278] that are highly variable between 2.5 mm per year (Afar) and 49.4 mm per year (Caroline), with Hawaii moving at a relatively low speed of 11.6 mm per year since 5 Ma. This same study also shows that the Pacific hotspots move at speeds between 10 and 50 mm per year, whereas Atlantic Ocean and Indian Ocean hotspots would move more slowly, below 20 mm per year. Yet another alternative kinematics-based approach was developed[280] to determine the motions of major hotspots for the last 80 million years by estimating misfits

at the same time as fitting hotspot tracks and treating all hotspots as fixed. The resulting hotspot trail misfits represent a robust estimate of hotspot motion, with rates generally below 40 mm per year for all major hotspots, except for Hawaii, which shows a mean rate of hotspot motion of ~24.1 mm per year over 80 million years, with maximum rates of ~92.8 mm per year between ~60 and 55 Ma and ~48.8 mm per year between ~50 and 45 Ma (REF.[280]). However, we note that for modelling present-day plate motions the best-fit, hotspot-defined absolute plate motion reference frames appear statistically similar for fixed and moving hotspot models[281]. In addition, other authors have used similar data (but only considered the azimuth of hotspot trends) and conclude that there is no requirement for hotspots — that are active at the present day — to move and that a fixed hotspot reference frame can fit the data better[282]. These contrasting papers exemplify the extent of the ongoing controversy about hotspot motion.

Importantly, these scenarios can now be compared with geodynamic models of hotspot motion within regimes of large-scale mantle flow[62,163,283] that can be computed based on density models inferred from 3D seismic tomography, assuming whole-mantle viscosity profiles, and time-dependent plate motions as surface boundary conditions. The approach is completed by inserting initially vertical plume conduits that are then advected while buoyantly rising through the convecting mantle. In these geodynamic models, the computed hotspot motions are typically slower than plate motions, mostly less than 10 mm per year, which is a consequence of plumes being anchored in and rising from the lower mantle, which is only sluggishly convecting because of its high viscosity[163] (up to about 10^{23} Pa s). This geodynamic modelling approach is most reliable in the Cenozoic, but less so for times prior to 50 Ma, as backward advection of mantle density anomalies becomes increasingly unreliable (BOX 2). Complementary to this approach are geodynamic forward models that can capture both the tilt of plume stems in the mantle as well as the motion of the plume generation zone[13,276].

Breaking up continents and initiating subduction. Mantle plumes can play an active role in the break-up of continents and/or oceanic lithosphere, when they impinge those from beneath, providing a starting point for the Wilson Cycle in plate tectonics and a likely important initiation mechanism for far-field major plate reorganizations[28,48,49]. Modelling suggests that, although the plume push force is transient, it can play a major role in the initial rifting[51]. Continental break-up occurs when enough extension occurs to split continental lithosphere and form a new ocean basin. Many of the continental flood basalt provinces in the Mesozoic and Cenozoic are closely related in time and space with continental break-up[1,48–50]. When reconstructed back to their original plate tectonic configuration, these flood basalt provinces are often found along continental margins, and dike swarms have more or less radial patterns and terminate at the margins of continental cratons[284,285].

These observations led to the active continental rift hypothesis, where mantle plumes are thought to drive continental break-up. In this model, continental rifting is actively driven by mantle plume processes, including arrival of a plume head at the base of the lithosphere, heating and erosion of the lithosphere, and heating, uplift and tensional failure of the mechanical lithosphere[48]. Alternatively, continental break-up can be explained by the passive rifting model, where continental rifting is driven by far-field tectonic forces and interaction with an existing plume is coincidental[286–288]. In both scenarios, the combination of lithospheric extension and upwelling plume material causes abnormally large volumes of magma to erupt through passive decompression melting[50]. It also appears that most continental rifts without a plume failed, with only one-third proceeding to break-up[289]. The fact that continental rifting can extend from only a few million years up to around 100 million years before progressing to continental break-up, therefore, has called for a combination of passive forces and active plume head forces[48].

For continental rifts that do proceed to break-up, plumes appear to play a triggering, but not an essential, role. The role for plumes is particularly striking when the timing of continental rifting, flood basalt eruption and continental break-up are compared, with continental rifting often extending for tens of millions of years and — after this prolonged period — ending with the voluminous eruption of flood basalts that are coevally, or closely followed by, continental break-up[290]. The role of plumes as a trigger for continental break-up has been tested by modelling lithosphere under far-field extension, investigating the role of plume-related lithospheric erosion[291]. It was found that plume erosion decreases lithospheric strength and controls the timing or even occurrence of continental break-up. Plumes can help to trigger final continental break-up by weakening lithosphere where it is already thinned, as hot plume material feeds into existing rifts and sutures, and plume-induced melts can thin even thick cratonic lithosphere and facilitate rifting[292,293].

Mantle plumes in combination with changes in plate boundary forces[294,295] and wrench tectonics[296] are also thought to drive the formation of microcontinents, small continental fragments that become separated from their parent continental margin and, eventually, are surrounded by oceanic lithosphere. In these smaller-scale manifestations of plate tectonics, mantle plumes have been implicated in the rifting and separating of microcontinents from relatively young continental margins, less than 25 million years old. Plume involvement in rifting is thought to happen through one or multiple mid-ocean-ridge relocations that are centred around the mantle plume, resulting in ocean-spreading asymmetries and ridge propagation towards the locus of the plume[297].

Whereas arc volcanism associated with subduction is thought to be the main process producing continental crust in modern-style plate tectonics, plume-associated volcanism has been invoked for heat transport and formation of continental crust in the early Earth[298,299]. In this sense, mantle plumes might be related to the initiation of oceanic subduction and, hence, modern plate tectonics, either indirectly by creating thick and buoyant continental crust that can initiate oceanic subduction by

Box 2 | **True polar wander**

Motion of the magnetic north pole as seen from a specific tectonic plate can be caused by plate motion (apparent polar wander) or by reorientation of the entire Earth relative to its geographic poles (true polar wander). For approximately the last 120 million years, plate motion can be determined from hotspot tracks, allowing a true polar wander path to be reconstructed by rotating a single plate back to its past locations in the hotspot reference frame, and transferring the corresponding palaeomagnetic pole positions for those past geological times with it. The remainder trace of past pole positions then, in theory, equals the true polar wander path for that tectonic plate. Individual true polar wander paths from different plates can be combined to devise a global true polar wander path, but they might show minor differences because of non-dipolar components of the magnetic field and other geological uncertainties[335,336]. Because true polar wander is expected from substantial shifts in Earth's mass distribution[337] on geological timescales, it is likely to result from major reconfigurations in large-scale mantle structures[338]. The two large low-shear-velocity province (LLSVP) superstructures beneath Africa and the mid-Pacific, however, are thought to have had a stabilizing effect over the last couple of hundreds of millions of years[128–130,339,340], whereby Earth's spin axis remained aligned with the geoid low that is present between the two antipodal geoid highs caused by the LLSVPs. In that configuration, true polar wander may still occur, but is restricted to a ring around the Earth that runs between the two LLSVPs, and it would be a process that is driven by the sinking of dense lithospheric slabs subducting mostly near that ring[341]. The largest amount of true polar wander that has been detected since 120 million years ago (Ma) and that follows this ring occurred at speeds on the order of 10 mm per year and between 100 and 110 Ma (REF.[341]). In addition, a high-resolution palaeomagnetic measurements for two overlapping stratigraphic limestone sections in Italy show evidence for ~12° of true polar wander between 86 and 78 Ma (REF.[342]), which confirms an earlier study that showed a comparable 16 ± 3° shift for the Pacific Plate around 84 Ma (REF.[343]).

The two modelled true polar wander paths shown in the figure are derived from (palaeo)magnetic results and only indicate minor true polar wander over the last 50 million years. The uncertainty ellipses representing 95% confidence shown in blue[283] and red[344] are relative to the global and Pacific hotspot reference frames, respectively.

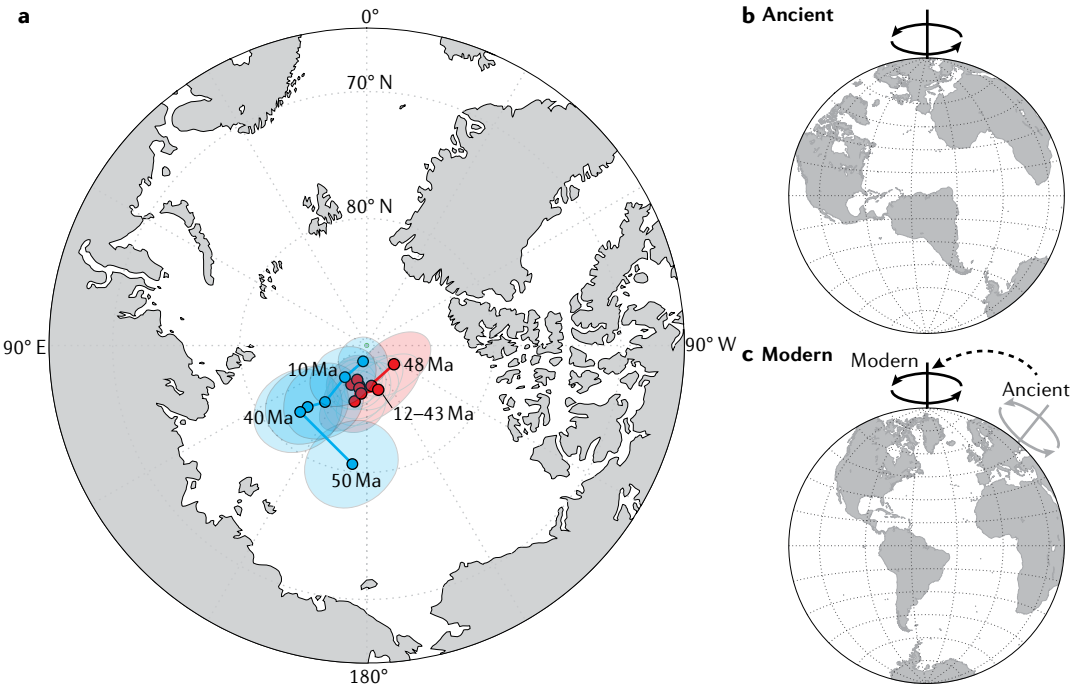

means of a lateral or a vertical density contrast[300–302] or directly through plume-related weakening[303].

Summary and future directions

Even though mantle plumes occur on different spatio-temporal scales from plate tectonic processes such as seafloor spreading and subduction, all are part of the large-scale thermochemical convection in Earth's mantle. Mantle plumes are a major component of the overall rock cycle in the Earth system, playing a key role in the continuous recycling of Earth's deep interior and surface materials. Many mantle plumes originate from the deepest regions in Earth's mantle, often in association with LLSVPs and ULVZs, and plumes potentially even take in material from the Earth's core itself. At Earth's surface, clear evidence of plume activity causing intra-plate volcanism, aiding continental break-up and triggering long-term effects on Earth's climate system might be seen. Yet, knowledge of mantle plumes remains limited, largely because of the low-resolution view we have of their structures and behaviours through seismic mantle tomography studies, and because of the complexity of plume expressions in the volcanic structures (seamount trails, oceanic plateaux) on Earth's surface. Below, we compile a short list of future research themes that could improve

understanding of mantle plumes themselves and their effects on the interconnected Earth system.

Deep mantle structure and plume nurseries. Reconciling current seismic images of mantle plumes with the geodynamic modelling and surface observations is a major challenge for the future. Large-scale deployments of ocean bottom seismometers with wider apertures are required to create detailed views of the deep portions of mantle plumes. For example, improvements on the design, geometries and placement of these instruments are needed to capture specific seismic phases that can better resolve structures at the roots of mantle plumes and shed light on their potential generation in LLSVP and ULVZ regions. These improvements in global seismic tomography are required to provide higher-resolution information (on 100-km scales or better) that can shed new light on the differences and nature of thermal and thermochemical plumes in the lower mantle. Higher-resolution tomography would also help to determine the relation between plumes and a potential basal dense layer, and would allow for the exploration of more complex mantle rheologies to explain plume morphologies and temporal behaviours. Increased tomography resolution is also needed to understand how plumes interact with the overall mantle flow and become deflected in the 660–1,000-km depth range.

An exciting and growing field of mantle geodynamics involves the generation of 3D spherical shell numerical models of the Earth that solve the governing equations for appropriate physical parameters and can include increasingly complex rheologies. These models can evolve through geological time, allowing us to study the interactions between tectonic processes, large-scale mantle flow and plumes[140,165,277,304,305]. The simulation output can then be used to improve the interpretation of complex seismic tomographic features. With advancements in supercomputing, it is expected that this style of 3D modelling will continue to advance and provide important insights into Earth's inner workings.

Of particular interest is to further examine whether transition zone plumes exist (plumes that are rooted in the mid-mantle, instead of the lower mantle). If so, it will be important to establish whether they occur as small offshoots from ponded lower mantle plumes[23,63,171], whether they start out as individual upwellings from the 660-km mantle discontinuity[24,44,61,63] or whether they are deep plumes getting (severely) deflected at the base of the extended transition zone at ~1,000-km depth[69,72]. Transition zone plumes could also be the natural consequence of asthenospheric convection related to the subduction process and slab-induced hydration of the transition zone[306].

Volcanic surface expressions. The formation and history of oceanic LIPs are still poorly understood compared with their extensively studied onshore counterparts. For example, there is an intriguing association with spreading ridges and triple junctions. Over the last decade, studies on Shatsky Rise[307,308] have reinforced the idea that some LIPs might not be caused by plume head eruptions, raising the question whether Shatsky and other LIPs are the result of headless plumes interacting with overriding oceanic spreading centres. Similarly, it will be important to establish whether Cretaceous LIPs existed that could have formed from plume heads belonging to, for example, the Hawaii and Louisville mantle plumes, which, by now, could have been obducted onto land[110] or subducted into the upper mantle[176].

Recording the entire spatiotemporal and chemical evolution of mantle plume systems will provide important testing for the plume head–tail hypothesis[27,28]. It will also offer insights into the cyclicities of global intra-plate volcanism — as, over the last 200 million years, a waxing and waning of global intra-plate volcanism[92,93] and ocean crust formation[309,310] has been observed — but drivers and potential links between these cyclicities remain unknown. Future research needs to provide process-based understanding whether plume formation through time can be linked to coupled plate tectonic and mantle evolution, such as cycles of plate aggregation, dispersal and subduction. Related to this is figuring out why plumes have such a wide range of lifespans (anything from ~30 to 150 million years and longer) and how their roles changed as a function of a decreasing internal heat production over Earth's history.

Mantle plume source regions. Over the last half a century, geochemical studies have led to a shift in the understanding of the make-up of the mantle from a homogeneous material body to a complex mix of mantle domains. Each of these domains is characterized by their own unique heritage and evolution (for example, through subduction or core–mantle interactions) and a range of geodynamic processes (including mixing and entrainment) that could have altered them. There are still limited ideas on the timescales and length scales of these domains, where they reside and what is their long-term stability. To address these outstanding issues, better efforts must be made to coordinate geochemical, isotopic and geochronological analyses on the same samples, especially for multiple novel, short-lived isotopic systems. For example, it is not known how ^{129}Xe anomalies observed in mantle plume source regions (which track the degassing history of the planet) relate to observed ^{182}W anomalies (which can track core formation)[311] because only one rock has, so far, been characterized for both ^{129}Xe and ^{182}W, but this sample is not (yet) characterized for ^{142}Nd (which tracks silicate Earth differentiation). Future advances will require an integrated multi-proxy geochemical and dating effort with coordination across laboratories.

Linking the geochemistry of ocean island lava flows to underlying mantle features is of primary geological importance. Hence, future improvements in understanding the variable make-up of the mantle requires joint geochemical, geodynamic and geophysical research at multiple global hotspots, including low-flux hotspots. It is important to focus on other hotspot systems in addition to Hawaii, as this plume's anomalously high buoyancy flux (relative to the global average for hotspots) and related higher melt flux have the potential to obscure geographic trends in plume-derived lava chemistry, which might be more easily discernible at low-flux hotspots[246].

Dynamic topography
The part of topography that is caused, supported and maintained by mantle convection.

Environmental impacts. The upwelling of mantle plumes can affect the dynamic topography of oceanic lithosphere[125,148,312–314]. Where the presence of strong or weak mantle plumes causes large or small hotspots swells[144] and regional modifications in mantle viscosity profiles, the pulsating behaviour of mantle plumes might cause substantial variations in local sea level that can change ocean circulation patterns and deep-sea sedimentation accumulation rates[148]. Gaps in understanding mantle viscosity profiles, especially in the proximity of larger plume swells, are causing major uncertainties in modelling future local sea level rise across the world[315–317]. Mantle plume activity also can result in extensive volcanism on Earth's surface, causing extreme global environmental perturbations and mass extinctions[52–54]. For example, the emplacement of the Deccan Traps flood basalt has been associated with the extinction at the Cretaceous–Palaeogene boundary (at ~66 Ma)[53,54,318–320] and the Siberian Traps have been associated with the most extensive mass extinction at the Permo–Triassic boundary (at ~250 Ma)[52,321–324]. In both cases, however, the timing and duration of volcanism has been debated in linking plume-generated volcanism to the extinctions[53,54,318,320–322]. Indeed, there are complex feedbacks and timing-related issues between mantle plumes, climate, coincident meteorite impacts and biosystems that remain the subject of debate[52,319,323–326]. A key challenge is to capture the complete chronologies that record the mantle plume events (such as flood basalts and oceanic plateaux) and to tie those to geological records that contain information about Earth's environment, species extinction, ocean chemistry, ocean acidification, oxygenation, meteorite impacts and more (such as terrestrial sedimentary records and sub-seafloor scientific ocean drill cores). Combining mantle plume and surface process records will enable discoveries on the importance of mantle plumes in solid Earth, climate and biosphere interactions, including their impacts on long-term climate change, mass extinctions and biosystem resiliency.

Published online: 25 May 2021

1. Morgan, W. J. Convection plumes in the lower mantle. *Nature* **230**, 42–43 (1971).
2. Wilson, J. T. A possible origin of the Hawaiian Islands. *Can. J. Phys.* **41**, 863–870 (1963).
3. Campbell, I. H. & Griffiths, R. W. Implications of mantle plume structure for the evolution of flood basalts. *Earth Planet. Sci. Lett.* **99**, 79–93 (1990).
4. Whitehead, J. A. & Luther, D. S. Dynamics of laboratory diapir and plume models. *J. Geophys. Res.* **80**, 705–717 (1975).
5. Hofmann, A. W. & White, W. M. Mantle plumes from ancient oceanic-crust. *Earth Planet. Sci. Lett.* **57**, 421–436 (1982).
6. White, W. M. & Hofmann, A. W. Sr and Nd isotope geochemistry of oceanic basalts and mantle evolution. *Nature* **296**, 821–825 (1982).
7. Zindler, A. & Hart, S. Chemical geodynamics. *Annu. Rev. Earth Planet. Sci.* **14**, 493–571 (1986).
8. Thorne, M. S., Garnero, E. J. & Grand, S. P. Geographic correlation between hot spots and deep mantle lateral shear-wave velocity gradients. *Phys. Earth Planet. Inter.* **146**, 47–63 (2004).
9. Boschi, L., Becker, T. W. & Steinberger, B. Mantle plumes: Dynamic models and seismic images. *Geochem. Geophys. Geosyst.* **8**, Q10006 (2007).
10. Tan, E., Leng, W., Zhong, S. J. & Gurnis, M. On the location of plumes and lateral movement of thermochemical structures with high bulk modulus in the 3-D compressible mantle. *Geochem. Geophys. Geosyst.* **12**, Q07005 (2011).
11. Steinberger, B. & Torsvik, T. H. A geodynamic model of plumes from the margins of Large Low Shear Velocity Provinces. *Geochem. Geophys. Geosyst.* **13**, Q01W09 (2012).
12. Davies, D. R., Goes, S. & Sambridge, M. On the relationship between volcanic hotspot locations, the reconstructed eruption sites of large igneous provinces and deep mantle seismic structure. *Earth Planet. Sci. Lett.* **411**, 121–130 (2015).
13. Hassan, R., Flament, N., Gurnis, M., Bower, D. J. & Muller, D. Provenance of plumes in global convection models. *Geochem. Geophys. Geosyst.* **16**, 1465–1489 (2015).
14. Austermann, J., Kaye, B. T., Mitrovica, J. X. & Huybers, P. A statistical analysis of the correlation between large igneous provinces and lower mantle seismic structure. *Geophys. J. Int.* **197**, 1–9 (2014).
15. Doubrovine, P. V., Steinberger, B. & Torsvik, T. H. A failure to reject: Testing the correlation between large igneous provinces and deep mantle structures with EDF statistics. *Geochem. Geophys. Geosyst.* **17**, 1130–1163 (2016).
16. Schubert, G., Turcotte, D. L. & Olson, P. *Mantle Convection in the Earth and Planets* (Cambridge Univ. Press, 2001).
17. Courtier, A. M., Bagley, B. & Revenaugh, J. Whole mantle discontinuity structure beneath Hawaii. *Geophys. Res. Lett.* **34**, L17304 (2007).
18. Putirka, K. Excess temperatures at ocean islands: Implications for mantle layering and convection. *Geology* **36**, 283–286 (2008).
19. Trela, J. et al. The hottest lavas of the Phanerozoic and the survival of deep Archaean reservoirs. *Nat. Geosci.* **10**, 451–45 (2017).
20. Moore, W. B., Schubert, G. & Tackley, P. Three-dimensional simulations of plume-lithosphere interaction at the Hawaiian swell. *Science* **279**, 1008–1011 (1998).
21. Ribe, N. M. & Christensen, U. R. The dynamical origin of Hawaiian volcanism. *Earth Planet. Sci. Lett.* **171**, 517–531 (1999).
22. Ballmer, M. D., Ito, G., van Hunen, J. & Tackley, P. J. Spatial and temporal variability in Hawaiian hotspot volcanism induced by small-scale convection. *Nat. Geosci.* **4**, 457–460 (2011).
23. Davaille, A. Simultaneous generation of hotspots and superswells by convection in a heterogeneous planetary mantle. *Nature* **402**, 756–760 (1999).
24. Davaille, A., Girard, F. & Le Bars, M. How to anchor hotspots in a convecting mantle? *Earth Planet. Sci. Lett.* **203**, 621–634 (2002).
25. Jellinek, A. M. & Manga, M. Links between long-lived hot spots, mantle plumes, D″, and plate tectonics. *Rev. Geophys.* **42**, RG3002 (2004).
26. Olson, P. & Yuen, D. A. Thermochemical plumes and mantle phase-transitions. *J. Geophys. Res.* **87**, 3993–4002 (1982).
27. Campbell, I. H., Griffiths, R. W. & Hill, R. I. Melting in an Archaean mantle plume: heads it's basalts, tails it's komatiites. *Nature* **339**, 697–699 (1989).
28. Richards, M. A., Duncan, R. A. & Courtillot, V. E. Flood basalts and hot-spot tracks: plume heads and tails. *Science* **246**, 103–107 (1989).
29. Allègre, C. J., Staudacher, T., Sarda, P. & Kurz, M. Constraints on evolution of Earth's mantle from rare gas systematics. *Nature* **303**, 762–766 (1983).
30. Koppers, A. A. P. & Watts, A. B. Intraplate seamounts as a window into deep Earth processes. *Oceanography* **23**, 42–57 (2010).
31. van der Meer, D. G., van Hinsbergen, D. J. J. & Spakman, W. Atlas of the underworld: Slab remnants in the mantle, their sinking history, and a new outlook on lower mantle viscosity. *Tectonophysics* **723**, 309–448 (2018).
32. Ricard, Y., Richards, M., Lithgowbertelloni, C. & Lestunff, Y. A geodynamic model of mantle density heterogeneity. *J. Geophys. Res. Solid Earth* **98**, 21895–21909 (1993).
33. Lithgow-Bertelloni, C. & Richards, M. A. The dynamics of Cenozoic and Mesozoic plate motions. *Rev. Geophys.* **36**, 27–78 (1998).
34. Mulyukova, E., Steinberger, B., Dabrowski, M. & Sobolev, S. V. Survival of LLSVPs for billions of years in a vigorously convecting mantle: Replenishment and destruction of chemical anomaly. *J. Geophys. Res. Solid Earth* **120**, 3824–3847 (2015).
35. Domeier, M., Doubrovine, P. V., Torsvik, T. H., Spakman, W. & Bull, A. L. Global correlation of lower mantle structure and past subduction. *Geophys. Res. Lett.* **43**, 4945–4953 (2016).
36. Dziewonski, A. M. & Woodhouse, J. H. Global images of the Earth's interior. *Science* **236**, 37–48 (1987).
37. Garnero, E. J., McNamara, A. K. & Shim, S. H. Continent-sized anomalous zones with low seismic velocity at the base of Earth's mantle. *Nat. Geosci.* **9**, 481–489 (2016).
38. Grand, S. P., van der Hilst, R. D. & Widiyantoro, S. High resolution global tomography: a snapshot of convection in the Earth. *GSA Today* **7** (1997).
39. Li, X. D. & Romanowicz, B. Global mantle shear velocity model developed using nonlinear asymptotic coupling theory. *J. Geophys. Res. Solid Earth* **101**, 22245–22272 (1996).
40. Masters, G., Laske, G., Bolton, H. & Dziewonski, A. The relative behavior of shear velocity, bulk sound speed, and compressional velocity in the mantle: Implications for chemical and thermal structure. *Geophys. Monogr. Ser.* **117**, 63–87 (2000).
41. Ritsema, J., Deuss, A., van Heijst, H. J. & Woodhouse, J. H. S40RTS: a degree-40 shear-velocity model for the mantle from new Rayleigh wave dispersion, teleseismic traveltime and normal-mode splitting function measurements. *Geophys. J. Int.* **184**, 1223–1236 (2011).
42. Su, W. J. & Dziewonski, A. M. Simultaneous inversion for 3-D variations in shear and bulk velocity in the mantle. *Phys. Earth Planet. Inter.* **100**, 135–156 (1997).
43. Li, M. M. & Zhong, S. J. The source location of mantle plumes from 3D spherical models of mantle convection. *Earth Planet. Sci. Lett.* **478**, 47–57 (2017).
44. Tan, E., Gurnis, M. & Han, L. J. Slabs in the lower mantle and their modulation of plume formation. *Geochem. Geophys. Geosyst.* **3**, 1–24 (2002).
45. Allègre, C. J. Chemical geodynamics. *Tectonophysics* **81**, 109–132 (1982).
46. Hart, S. R. Heterogeneous mantle domains: signatures, genesis and mixing chronologies. *Earth Planet. Sci. Lett.* **90**, 273–296 (1988).
47. Stracke, A. Earth's heterogeneous mantle: A product of convection-driven interaction between crust and mantle. *Chem. Geol.* **330**, 274–299 (2012).
48. Courtillot, V., Jaupart, C., Manighetti, I., Tapponnier, P. & Besse, J. On causal links between flood basalts and continental breakup. *Earth Planet. Sci. Lett.* **166**, 177–195 (1999).
49. Storey, B. C. The role of mantle plumes in continental breakup: case histories from Gondwanaland. *Nature* **377**, 301–308 (1995).
50. White, R. & Mckenzie, D. Magmatism at rift zones: the generation of volcanic continental margins and flood basalts. *J. Geophys. Res. Solid Earth* **94**, 7685–7729 (1989).

51. Zhang, N., Dang, Z., Huang, C. & Li, Z. X. The dominant driving force for supercontinent breakup: Plume push or subduction retreat? *Geosci. Front.* **9**, 997–1007 (2018).
52. Courtillot, V. & Fluteau, F. in *Volcanism, Impacts, and Mass Extinctions: Causes and Effects* Vol. 505 (eds Keller, G. & Kerr, A. C.) 301–317 (Geological Society of America, 2014).
53. Duncan, R. A. & Pyle, D. G. Rapid eruption of the Deccan flood basalts at the Cretaceous/Tertiary boundary. *Nature* **333**, 841–843 (1988).
54. Renne, P. R. et al. Time scales of critical events around the Cretaceous-Paleogene boundary. *Science* **339**, 684–687 (2013).
55. Anderson, D. L. The persistent mantle plume myth. *Aust. J. Earth Sci.* **60**, 657–673 (2013).
56. Anderson, D. L. & Natland, J. H. Mantle updrafts and mechanisms of oceanic volcanism. *Proc. Natl Acad. Sci. USA* **111**, E4298–E4304 (2014).
57. Sleep, N. H. Hotspots and mantle plumes: Some phenomenology. *J. Geophys. Res. Solid Earth* **95**, 6715–6736 (1990).
58. Sleep, N. H. Mantle plumes from top to bottom. *Earth Sci. Rev.* **77**, 231–271 (2006).
59. van Keken, P. Evolution of starting mantle plumes: a comparison between numerical and laboratory models. *Earth Planet. Sci. Lett.* **148**, 1–11 (1997).
60. Konrad, K. et al. On the relative motions of long-lived Pacific mantle plumes. *Nat. Commun.* **9**, 854 (2018).
61. Koppers, A. A. P. Mantle plumes persevere. *Nat. Geosci.* **4**, 816–817 (2011).
62. Steinberger, B. Plumes in a convecting mantle: Models and observations for individual hotspots. *J. Geophys. Res. Solid Earth* **105**, 11127–11152 (2000).
63. Courtillot, V., Davaille, A., Besse, J. & Stock, J. Three distinct types of hotspots in the Earth's mantle. *Earth Planet. Sci. Lett.* **205**, 295–308 (2003).
64. Schubert, G., Masters, G., Olson, P. & Tackley, P. Superplumes or plume clusters? *Phys. Earth Planet. Inter.* **146**, 147–162 (2004).
65. Sandwell, D. T. et al. Evidence for diffuse extension of the Pacific plate from Pukapuka ridges and cross-grain gravity lineations. *J. Geophys. Res. Solid. Earth* **100**, 15087–15099 (1995).
66. Foulger, G. R. & Natland, J. H. Is "hotspot" volcanism a consequence of plate tectonics? *Science* **300**, 921–922 (2003).
67. Foulger, G. R. Origin of the South Atlantic igneous province. *J. Volcanol. Geotherm. Res.* **355**, 2–20 (2018).
68. Montelli, R., Nolet, G., Dahlen, F. A. & Masters, G. A catalogue of deep mantle plumes: New results from finite-frequency tomography. *Geochem. Geophys. Geosyst.* **7**, Q11007 (2006).
69. Lei, W. et al. Global adjoint tomography—model GLAD-M25. *Geophys. J. Int.* **223**, 1–21 (2020).
70. Zhao, D. P. Global tomographic images of mantle plumes and subducting slabs: insight into deep Earth dynamics. *Phys. Earth Planet. Inter.* **146**, 3–34 (2004).
71. Boschi, L., Becker, T. W. & Steinberger, B. On the statistical significance of correlations between synthetic mantle plumes and tomographic models. *Phys. Earth Planet. Inter.* **167**, 230–238 (2008).
72. French, S. W. & Romanowicz, B. Broad plumes rooted at the base of the Earth's mantle beneath major hotspots. *Nature* **525**, 95–99 (2015).
73. Nelson, P. L. & Grand, S. P. Lower-mantle plume beneath the Yellowstone hotspot revealed by core waves. *Nat. Geosci.* **11**, 280–28 (2018).
74. White, W. M. Oceanic island basalts and mantle plumes: the geochemical perspective. *Annu. Rev. Earth Planet. Sci.* **38**, 133–160 (2010).
75. Jackson, M. G., Becker, T. W. & Konter, J. G. Geochemistry and distribution of recycled domains in the mantle inferred from Nd and Pb isotopes in oceanic hot spots: Implications for storage in the large low shear wave velocity provinces. *Geochem. Geophys. Geosyst.* **19**, 3496–3519 (2018).
76. Abouchami, W. et al. Lead isotopes reveal bilateral asymmetry and vertical continuity in the Hawaiian mantle plume. *Nature* **434**, 851–856 (2005).
77. Dannberg, J. & Gassmoller, R. Chemical trends in ocean islands explained by plume–slab interaction. *Proc. Natl Acad. Sci. USA* **115**, 4351–4356 (2018).
78. Farnetani, C. G. & Hofmann, A. W. Dynamics and internal structure of the Hawaiian plume. *Earth Planet. Sci. Lett.* **295**, 231–240 (2010).
79. Hoernle, K. et al. How and when plume zonation appeared during the 132 Myr evolution of the Tristan Hotspot. *Nat. Commun.* **6**, 7799 (2015).
80. Hofmann, A. W. & Farnetani, C. G. Two views of Hawaiian plume structure. *Geochem. Geophys. Geosyst.* **14**, 5308–5322 (2013).
81. Huang, S. C., Hall, P. S. & Jackson, M. G. Geochemical zoning of volcanic chains associated with Pacific hotspots. *Nat. Geosci.* **4**, 874–878 (2011).
82. Weis, D., Garcia, M. O., Rhodes, J. M., Jellinek, M. & Scoates, J. S. Role of the deep mantle in generating the compositional asymmetry of the Hawaiian mantle plume. *Nat. Geosci.* **4**, 831–838 (2011).
83. Mukhopadhyay, S. Early differentiation and volatile accretion recorded in deep-mantle neon and xenon. *Nature* **486**, 101–104 (2012).
84. Peters, B. J., Carlson, R. W., Day, J. M. D. & Horan, M. F. Hadean silicate differentiation preserved by anomalous $^{142}Nd/^{144}Nd$ ratios in the Réunion hotspot source. *Nature* **555**, 89–93 (2018).
85. Mukhopadhyay, S. & Parai, R. Noble gases: a record of Earth's evolution and mantle dynamics. *Annu. Rev. Earth Planet. Sci.* **47**, 389–419 (2019).
86. Rizo, H. et al. ^{182}W evidence for core-mantle interaction in the source of mantle plumes. *Geochem. Perspect. Lett.* **11**, 6–11 (2019).
87. Mundl-Petermeier, A. et al. Anomalous ^{182}W in high $^{3}He/^{4}He$ ocean island basalts: Fingerprints of Earth's core? *Geochim. Cosmochim. Acta* **271**, 194–211 (2020).
88. Dziewonski, A. M., Hager, B. H. & O'Connell, R. J. Large-scale heterogeneities in the lower mantle. *J. Geophys. Res.* **82**, 239–255 (1977).
89. Hager, B. H., Clayton, R. W., Richards, M. A., Comer, R. P. & Dziewonski, A. M. Lower mantle heterogeneity, dynamic topography and the geoid. *Nature* **313**, 541–546 (1985).
90. Davies, G. F. Ocean bathymetry and mantle convection: 1. Large-scale flow and hotspots. *J. Geophys. Res. Solid Earth* **93**, 10467–10480 (1988).
91. Richards, M. A., Hager, B. H. & Sleep, N. H. Dynamically supported geoid highs over hotspots: Observation and theory. *J. Geophys. Res. Solid Earth* **93**, 7690–7708 (1988).
92. Larson, R. L. Geological consequences of superplumes. *Geology* **19**, 963–966 (1991).
93. Larson, R. L. Latest pulse of Earth: Evidence for a mid-Cretaceous superplume. *Geology* **19**, 547–550 (1991).
94. McNutt, M. K. Superswells. *Rev. Geophys.* **36**, 211–244 (1998).
95. Anderson, D. L. Hotspots, polar wander, Mesozoic convection and the geoid. *Nature* **297**, 391–393 (1982).
96. Richards, M. A. & Engebretson, D. C. Large-scale mantle convection and the history of subduction. *Nature* **355**, 437–440 (1992).
97. van der Hilst, R. D., Widiyantoro, S. & Engdahl, E. R. Evidence for deep mantle circulation from global tomography. *Nature* **386**, 578–584 (1997).
98. Ritsema, J. & Lekić, V. Heterogeneity of seismic wave velocity in Earth's mantle. *Annu. Rev. Earth Planet. Sci.* **48**, 377–401 (2020).
99. Becker, T. W. & Boschi, L. A comparison of tomographic and geodynamic mantle models. *Geochem. Geophys. Geosyst.* **3**, 2001GC000168 (2002).
100. Lekic, V., Cottaar, S., Dziewonski, A. & Romanowicz, B. Cluster analysis of global lower mantle tomography: A new class of structure and implications for chemical heterogeneity. *Earth Planet. Sci. Lett.* **357**, 68–77 (2012).
101. Kennett, B. L. N., Widiyantoro, S. & van der Hilst, R. D. Joint seismic tomography for bulk sound and shear wave speed in the Earth's mantle. *J. Geophys. Res. Solid Earth* **103**, 12469–12493 (1998).
102. Deschamps, F., Cobden, L. & Tackley, P. J. The primitive nature of large low shear-wave velocity provinces. *Earth Planet. Sci. Lett.* **349**, 198–208 (2012).
103. Ni, S., Tan, E., Gurnis, M. & Helmberger, D. Sharp sides to the African superplume. *Science* **296**, 1850–1852 (2002).
104. Wang, Y. & Wen, L. X. Mapping the geometry and geographic distribution of a very low velocity province at the base of the Earth's mantle. *J. Geophys. Res. Solid Earth* **109**, B10305 (2004).
105. To, A., Romanowicz, B., Capdeville, Y. & Takeuchi, N. 3D effects of sharp boundaries at the borders of the African and Pacific Superplumes: Observation and modeling. *Earth Planet. Sci. Lett.* **233**, 137–153 (2005).
106. Davies, D. R. et al. Reconciling dynamic and seismic models of Earth's lower mantle: The dominant role of thermal heterogeneity. *Earth Planet. Sci. Lett.* **353**, 253–269 (2012).
107. Schuberth, B. S. A., Bunge, H. P. & Ritsema, J. Tomographic filtering of high-resolution mantle circulation models: Can seismic heterogeneity be explained by temperature alone?. *Geochem. Geophys. Geosyst.* **10**, Q05W03 (2009).
108. Ishii, M. & Tromp, J. Constraining large-scale mantle heterogeneity using mantle and inner-core sensitive normal modes. *Phys. Earth Planet. Inter.* **146**, 113–124 (2004).
109. Simmons, N. A., Forte, A. M., Boschi, L. & Grand, S. P. GyPSuM: A joint tomographic model of mantle density and seismic wave speeds. *J. Geophys. Res. Solid Earth* **115**, B12310 (2010).
110. Niu, Y. Origin of the LLSVPs at the base of the mantle is a consequence of plate tectonics – A petrological and geochemical perspective. *Geosci. Front.* **9**, 1265–1278 (2018).
111. Ballmer, M. D., Schumacher, L., Lekic, V., Thomas, C. & Ito, G. Compositional layering within the large low shear-wave velocity provinces in the lower mantle. *Geochem. Geophys. Geosyst.* **17**, 5056–5077 (2016).
112. Romanowicz, B. Can we resolve 3D density heterogeneity in the lower mantle? *Geophys. Res. Lett.* **28**, 1107–1110 (2001).
113. Trampert, J., Deschamps, F., Resovsky, J. & Yuen, D. Probabilistic tomography maps chemical heterogeneities throughout the lower mantle. *Science* **306**, 853–856 (2004).
114. Akbarashrafi, F., Al-Attar, D., Deuss, A., Trampert, J. & Valentine, A. P. Exact free oscillation spectra, splitting functions and the resolvability of Earth's density structure. *Geophys. J. Int.* **213**, 58–76 (2018).
115. Lau, H. C. P. et al. Tidal tomography constrains Earth's deep-mantle buoyancy. *Nature* **551**, 321–326 (2017).
116. Koelemeijer, P., Deuss, A. & Ritsema, J. Density structure of Earth's lowermost mantle from Stoneley mode splitting observations. *Nat. Commun.* **8**, 15241 (2017).
117. McNamara, A. K. A review of large low shear velocity provinces and ultra low velocity zones. *Tectonophysics* **760**, 199–220 (2019).
118. Macpherson, C. G., Hilton, D. R., Sinton, J. M., Poreda, R. J. & Craig, H. High $^{3}He/^{4}He$ ratios in the Manus backarc basin: Implications for mantle mixing and the origin of plumes in the western Pacific Ocean. *Geology* **26**, 1007–1010 (1998).
119. Williams, C. D., Mukhopadhyay, S., Rudolph, M. L. & Romanowicz, B. Primitive helium is sourced from seismically slow regions in the lowermost mantle. *Geochem. Geophys. Geosyst.* **20**, 4130–4145 (2019).
120. Mundl, A. et al. Tungsten-182 heterogeneity in modern ocean island basalts. *Science* **356**, 66–69 (2017).
121. Mundl-Petermeier, A. et al. Temporal evolution of primordial tungsten-182 and $^{3}He/^{4}He$ signatures in the Iceland mantle plume. *Chem. Geol.* **525**, 245–259 (2019).
122. McNamara, A. K. & Zhong, S. Thermochemical structures beneath Africa and the Pacific Ocean. *Nature* **437**, 1136–1139 (2005).
123. Davaille, A. & Romanowicz, B. Deflating the LLSVPs: bundles of mantle thermochemical plumes rather than thick stagnant "piles". *Tectonics* **39**, e2020TC006265 (2020).
124. Bull, A. L., Domeier, M. & Torsvik, T. H. The effect of plate motion history on the longevity of deep mantle heterogeneities. *Earth Planet. Sci. Lett.* **401**, 172–182 (2014).
125. Zhang, N., Zhong, S. J., Leng, W. & Li, Z. X. A model for the evolution of the Earth's mantle structure since the Early Paleozoic. *J. Geophys. Res. Solid Earth* **115**, B06401 (2010).
126. Heron, P. J. et al. Ancient subducted oceans controlling the positioning of deep mantle plumes. Preprint at *EarthArXiv* 10.31223/osf.io/vdmys (2019)..
127. Frost, D. A. & Rost, S. The P-wave boundary of the large-low shear velocity province beneath the Pacific. *Earth Planet. Sci. Lett.* **403**, 380–392 (2014).
128. Burke, K. & Torsvik, T. H. Derivation of large igneous provinces of the past 200 million years from long-term heterogeneities in the deep mantle. *Earth Planet. Sci. Lett.* **227**, 531–538 (2004).
129. Torsvik, T. H., Smethurst, M. A., Burke, K. & Steinberger, B. Large igneous provinces generated from the margins of the large low-velocity provinces in the deep mantle. *Geophys. J. Int.* **167**, 1447–1460 (2006).
130. Burke, K., Steinberger, B., Torsvik, T. H. & Smethurst, M. A. Plume generation zones at the margins of large low shear velocity provinces on the core–mantle boundary. *Earth Planet. Sci. Lett.* **265**, 49–60 (2008).

131. Cottaar, S. & Romanowicz, B. An unsually large ULVZ at the base of the mantle near Hawaii. *Earth Planet. Sci. Lett.* **355**, 213–222 (2012).
132. Thorne, M. S., Garnero, E. J., Jahnke, G., Igel, H. & McNamara, A. K. Mega ultra low velocity zone and mantle flow. *Earth Planet. Sci. Lett.* **364**, 59–67 (2013).
133. Yuan, K. Q. & Romanowicz, B. Seismic evidence for partial melting at the root of major hot spot plumes. *Science* **357**, 393–396 (2017).
134. Kim, D., Lekic, V., Menard, B., Baron, D. & Taghizadeh-Popp, M. Sequencing seismograms: A panoptic view of scattering in the core-mantle boundary region. *Science* **368**, 1223–1228 (2020).
135. Rost, S., Garnero, E. J., Williams, Q. & Manga, M. Seismological constraints on a possible plume root at the core–mantle boundary. *Nature* **435**, 666–669 (2005).
136. Williams, Q. & Garnero, E. J. Seismic evidence for partial melt at the base of Earth's mantle. *Science* **273**, 1528–1530 (1996).
137. Mao, W. L. et al. Iron-rich post-perovskite and the origin of ultralow-velocity zones. *Science* **312**, 564–565 (2006).
138. Wicks, J. K., Jackson, J. M., Sturhahn, W. & Zhang, D. Z. Sound velocity and density of magnesiowustites: Implications for ultralow-velocity zone topography. *Geophys. Res. Lett.* **44**, 2148–2158 (2017).
139. Olson, P. & Kincaid, C. Experiments on the interaction of thermal convection and compositional layering at the base of the mantle. *J. Geophys. Res. Solid. Earth* **96**, 4347–4354 (1991).
140. Zhong, S. Constraints on thermochemical convection of the mantle from plume heat flux, plume excess temperature, and upper mantle temperature. *J. Geophys. Res. Solid Earth* **111**, B04409 (2006).
141. Coffin, M. F. & Eldholm, O. Large igneous provinces: crustal structure, dimensions, and external consequences. *Rev. Geophys.* **32**, 1–36 (1994).
142. Campbell, I. H. Testing the plume theory. *Chem. Geol.* **241**, 153–176 (2007).
143. Albers, M. & Christensen, U. R. The excess temperature of plumes rising from the core-mantle boundary. *Geophys. Res. Lett.* **23**, 3567–3570 (1996).
144. King, S. D. & Adam, C. Hotspot swells revisited. *Phys. Earth Planet. Inter.* **235**, 66–83 (2014).
145. Davies, G. F. Temporal variation of the Hawaiian plume flux. *Earth Planet. Sci. Lett.* **113**, 277–286 (1992).
146. Schilling, J.-G. Fluxes and excess temperatures of mantle plumes inferred from their interaction with migrating mid-ocean ridges. *Nature* **352**, 397–403 (1991).
147. Ito, G., Lin, J. & Gable, C. W. Interaction of mantle plumes and migrating mid-ocean ridges: Implications for the Galapagos plume-ridge system. *J. Geophys. Res. Solid Earth* **102**, 15403–15417 (1997).
148. Parnell-Turner, R. et al. A continuous 55-million-year record of transient mantle plume activity beneath Iceland. *Nat. Geosci.* **7**, 914–919 (2014).
149. Steinberger, B., Spakman, W., Japsen, P. & Torsvik, T. H. The key role of global solid-Earth processes in preconditioning Greenland's glaciation since the Pliocene. *Terra Nova* **27**, 1–8 (2015).
150. Lin, S. C. & van Keken, P. E. Dynamics of thermochemical plumes: 1. Plume formation and entrainment of a dense layer. *Geochem. Geophys. Geosyst.* **7**, Q02006 (2006).
151. McNamara, A. K. & Zhong, S. J. Thermochemical structures within a spherical mantle: Superplumes or piles?. *J. Geophys. Res. Solid Earth* **109**, B07402 (2004).
152. Farnetani, C. G. Excess temperature of mantle plumes: The role of chemical stratification across D″. *Geophys. Res. Lett.* **24**, 1583–1586 (1997).
153. Farnetani, C. G. & Samuel, H. Beyond the thermal plume paradigm. *Geophys. Res. Lett.* **32**, L07311 (2005).
154. Lin, S. C. & van Keken, P. E. Dynamics of thermochemical plumes: 2. Complexity of plume structures and its implications for mapping mantle plumes. *Geochem. Geophys. Geosyst.* **7**, Q03003 (2006).
155. Kumagai, I., Davaille, A., Kurita, K. & Stutzmann, E. Mantle plumes: Thin, fat, successful, or failing? Constraints to explain hot spot volcanism through time and space. *Geophys. Res. Lett.* **35**, L16301 (2008).
156. Dannberg, J. & Sobolev, S. V. Low-buoyancy thermochemical plumes resolve controversy of classical mantle plume concept. *Nat. Commun.* **6**, 6960 (2015).
157. Ballmer, M. D., Ito, G., Wolfe, C. J. & Solomon, S. C. Double layering of a thermochemical plume in the upper mantle beneath Hawaii. *Earth Planet. Sci. Lett.* **376**, 155–164 (2013).
158. Larsen, T. B. & Yuen, D. A. Fast plumeheads: Temperature-dependent versus non-Newtonian rheology. *Geophys. Res. Lett.* **24**, 1995–1998 (1997).
159. Torsvik, T. H. et al. Deep mantle structure as a reference frame for movements in and on the Earth. *Proc. Natl Acad. Sci. USA* **111**, 8735–8740 (2014).
160. Steinberger, B., Nelson, P. L., Grand, S. P. & Wang, W. Yellowstone plume conduit tilt caused by large-scale mantle flow. *Geochem. Geophys. Geosyst.* **20**, 5896–5912 (2019).
161. Butterworth, N. P. et al. Geological, tomographic, kinematic and geodynamic constraints on the dynamics of sinking slabs. *J. Geodyn.* **73**, 1–13 (2014).
162. Steinberger, B., Torsvik, T. H. & Becker, T. W. Subduction to the lower mantle–a comparison between geodynamic and tomographic models. *Solid. Earth* **3**, 415–432 (2012).
163. Steinberger, B. & O'Connell, R. J. Advection of plumes in mantle flow: implications for hotspot motion, mantle viscosity and plume distribution. *Geophys. J. Int.* **132**, 412–434 (1998).
164. Richards, M. A. & Griffiths, R. W. Deflection of plumes by mantle shear flow: experimental results and a simple theory. *Geophys. J.* **94**, 367–376 (1988).
165. Zhong, S. J., Zuber, M. T., Moresi, L. & Gurnis, M. Role of temperature-dependent viscosity and surface plates in spherical shell models of mantle convection. *J. Geophys. Res. Solid Earth* **105**, 11063–11082 (2000).
166. Koppers, A. A. P. et al. Limited latitudinal mantle plume motion for the Louisville hotspot. *Nat. Geosci.* **5**, 911–917 (2012).
167. Peate, D. W. in *Large Igneous Provinces: Continental, Oceanic and Planetary Flood Volcanism* Vol. 100 (eds Mahoney, J. J. & Coffin, M. F.) 217–245 (American Geophysical Union, 1997).
168. Ernst, R. E. & Buchan, K. L. Recognizing mantle plumes in the geological record. *Annu. Rev. Earth Planet. Sci.* **31**, 469–523 (2003).
169. Koppers, A. A. P., Morgan, J. P., Morgan, J. W. & Staudigel, H. Testing the fixed hotspot hypothesis using $^{40}Ar/^{39}Ar$ age progressions along seamount trails. *Earth Planet. Sci. Lett.* **185**, 237–252 (2001).
170. Tejada, M. L. G. et al. Geochemistry and age of Shatsky, Hess, and Ojin Rise seamounts: Implications for a connection between the Shatsky and Hess Rises. *Geochim. Cosmochim. Acta* **185**, 302–327 (2016).
171. Koppers, A. A. P., Staudigel, H., Pringle, M. S. & Wijbrans, J. R. Short-lived and discontinuous intraplate volcanism in the South Pacific: Hot spots or extensional volcanism?. *Geochem. Geophys. Geosyst.* **4**, 1089 (2003).
172. Clouard, V. & Bonneville, A. How many Pacific hotspots are fed by deep-mantle plumes? *Geology* **29**, 695–698 (2001).
173. Whitehead, J. A. Instabilities of fluid conduits in a flowing earth—are plates lubricated by the asthenosphere? *Geophys. J. Int.* **70**, 415–433 (1982).
174. Bercovici, D. & Mahoney, J. Double flood basalts and plume head separation at the 660-kilometer discontinuity. *Science* **266**, 1367–1369 (1994).
175. Niu, Y. L. et al. Testing the mantle plume hypothesis: an IODP effort to drill into the Kamchatka-Okhotsk Sea basement. *Sci. Bull.* **62**, 1464–1472 (2017).
176. Wei, S. S., Shearer, P. M., Lithgow-Bertelloni, C., Stixrude, L. & Tian, D. Oceanic plateau of the Hawaiian mantle plume head subducted to the uppermost lower mantle. *Science* **370**, 983–987 (2020).
177. Steinberger, B. & Antretter, M. Conduit diameter and buoyant rising speed of mantle plumes: Implications for the motion of hot spots and shape of plume conduits. *Geochem. Geophys. Geosyst.* **7**, Q11018 (2006).
178. Maguire, R., Ritsema, J., Bonnin, M., van Keken, P. E. & Goes, S. Evaluating the resolution of deep mantle plumes in teleseismic traveltime tomography. *J. Geophys. Res. Solid Earth* **123**, 384–400 (2018).
179. Maguire, R., Ritsema, J., van Keken, P. E., Fichtner, A. & Goes, S. P- and S-wave delays caused by thermal plumes. *Geophys. J. Int.* **206**, 1169–1178 (2016).
180. Ritsema, J. & Allen, R. M. The elusive mantle plume. *Earth Planet. Sci. Lett.* **207**, 1–12 (2003).
181. Stockmann, F., Cobden, L., Deschamps, F., Fichtner, A. & Thomas, C. Investigating the seismic structure and visibility of dynamic plume models with seismic array methods. *Geophys. J. Int.* **219**, S167–S194 (2019).
182. Nolet, G., Dahlen, F. & Montelli, R. Traveltimes and amplitudes of seismic waves: a re-assessment. *Geophys. Monogr. Ser.* **157**, 37 (2005).
183. Bijwaard, H. & Spakman, W. Tomographic evidence for a narrow whole mantle plume below Iceland. *Earth Planet. Sci. Lett.* **166**, 121–126 (1999).
184. Zhao, D. Seismic structure and origin of hotspots and mantle plumes. *Earth Planet. Sci. Lett.* **192**, 251–265 (2001).
185. Wolfe, C. J., Bjarnason, I. T., VanDecar, J. C. & Solomon, S. C. Seismic structure of the Iceland mantle plume. *Nature* **385**, 245–247 (1997).
186. Allen, R. M. et al. Plume-driven plumbing and crustal formation in Iceland. *J. Geophys. Res. Solid Earth* **107**, ESE 4-1–ESE 4-19 (2002).
187. Montelli, R. et al. Finite-frequency tomography reveals a variety of plumes in the mantle. *Science* **303**, 338–343 (2004).
188. Wolfe, C. J. et al. Mantle shear-wave velocity structure beneath the Hawaiian hot spot. *Science* **326**, 1388–1390 (2009).
189. Davaille, A., Carrez, P. & Cordier, P. Fat plumes may reflect the complex rheology of the lower mantle. *Geophys. Res. Lett.* **45**, 1349–1354 (2018).
190. Fukao, Y. & Obayashi, M. Subducted slabs stagnant above, penetrating through, and trapped below the 660 km discontinuity. *J. Geophys. Res. Solid Earth* **118**, 5920–5938 (2013).
191. Rudolph, M. L., Lekic, V. & Lithgow-Bertelloni, C. Viscosity jump in Earth's mid-mantle. *Science* **350**, 1349–1352 (2015).
192. Boschi, L. & Becker, T. W. Vertical coherence in mantle heterogeneity from global seismic data. *Geophys. Res. Lett.* **38**, L20306 (2011).
193. King, S. D. & Masters, G. An inversion for radial viscosity structure using seismic tomography. *Geophys. Res. Lett.* **19**, 1551–1554 (1992).
194. Mitrovica, J. X. & Forte, A. M. A new inference of mantle viscosity based upon joint inversion of convection and glacial isostatic adjustment data. *Earth Planet. Sci. Lett.* **225**, 177–189 (2004).
195. Jackson, M. G., Becker, T. W. & Steinberger, B. Spatial characteristics of recycled and primordial reservoirs in the deep mantle. *Geochem. Geophys. Geosyst.* **22**, e2020GC009525 (2021).
196. Jackson, M. G., Konter, J. G. & Becker, T. W. Primordial helium entrained by the hottest mantle plumes. *Nature* **542**, 340–343 (2017).
197. Chang, S.-J., Kendall, E., Davaille, A. & Ferreira, A. M. G. The evolution of mantle plumes in East Africa. *J. Geophys. Res. Solid Earth* **125**, e2020JB019929 (2020).
198. Halliday, A. N. Mixing, volatile loss and compositional change during impact-driven accretion of the Earth. *Nature* **427**, 505–509 (2004).
199. Carlson, R. W. & Boyet, M. Short-lived radionuclides as monitors of early crust–mantle differentiation on the terrestrial planets. *Earth Planet. Sci. Lett.* **279**, 147–156 (2009).
200. Horan, M. F. et al. Tracking Hadean processes in modern basalts with 142-Neodymium. *Earth Planet. Sci. Lett.* **484**, 184–191 (2018).
201. Kruijer, T. S. & Kleine, T. No ^{182}W excess in the Ontong Java Plateau source. *Chem. Geol.* **485**, 24–31 (2018).
202. Kurz, M. D., Jenkins, W. J. & Hart, S. R. Helium isotopic systematics of oceanic islands and mantle heterogeneity. *Nature* **297**, 43–47 (1982).
203. Willbold, M., Elliott, T. & Moorbath, S. The tungsten isotopic composition of the Earth's mantle before the terminal bombardment. *Nature* **477**, 195–198 (2011).
204. Puchtel, I. S., Blichert-Toft, J., Touboul, M., Horan, M. F. & Walker, R. J. The coupled ^{182}W-^{142}Nd record of early terrestrial mantle differentiation. *Geochem. Geophys. Geosyst.* **17**, 2168–2193 (2016).
205. Huang, S. C., Farkas, J. & Jacobsen, S. B. Stable calcium isotopic compositions of Hawaiian shield lavas: Evidence for recycling of ancient marine carbonates into the mantle. *Geochim. Cosmochim. Acta* **75**, 4987–4997 (2011).
206. Eiler, J. M., Farley, K. A., Valley, J. W., Hofmann, A. W. & Stolper, E. M. Oxygen isotope constraints on the sources of Hawaiian volcanism. *Earth Planet. Sci. Lett.* **144**, 453–467 (1996).
207. Cabral, R. A. et al. Anomalous sulphur isotopes in plume lavas reveal deep mantle storage of Archaean crust. *Nature* **496**, 490–493 (2013).
208. Konter, J. G. et al. Unusual $\delta^{56}Fe$ values in Samoan rejuvenated lavas generated in the mantle. *Earth Planet. Sci. Lett.* **450**, 221–232 (2016).

209. Nebel, O. et al. Reconciling petrological and isotopic mixing mechanisms in the Pitcairn mantle plume using stable Fe isotopes. *Earth Planet. Sci. Lett.* **521**, 60–67 (2019).
210. Gleeson, M. L. M., Gibson, S. A. & Williams, H. M. Novel insights from Fe-isotopes into the lithological heterogeneity of Ocean Island Basalts and plume-influenced MORBs. *Earth Planet. Sci. Lett.* **535**, 116114 (2020).
211. Harpp, K. S. & White, W. M. Tracing a mantle plume: Isotopic and trace element variations of Galapagos seamounts. *Geochem. Geophys. Geosyst.* **2**, 2000GC000137 (2001).
212. Hoernle, K. et al. Existence of complex spatial zonation in the Galápagos plume. *Geology* **28**, 435–438 (2000).
213. Jackson, M. G. et al. Helium and lead isotopes reveal the geochemical geometry of the Samoan plume. *Nature* **514**, 355–358 (2014).
214. Hawkesworth, C. J., Norry, M. J., Roddick, J. C. & Vollmer, R. $^{143}Nd/^{144}Nd$ and $^{87}Sr/^{86}Sr$ ratios from the Azores and their significance in LIL-element enriched mantle. *Nature* **280**, 28–31 (1979).
215. Jackson, M. G. et al. The return of subducted continental crust in Samoan lavas. *Nature* **448**, 684–687 (2007).
216. Chauvel, C., Hofmann, A. W. & Vidal, P. HIMU-EM: The French Polynesian connection. *Earth Planet. Sci. Lett.* **110**, 99–119 (1992).
217. Eisele, J. et al. The role of sediment recycling in EM-1 inferred from Os, Pb, Hf, Nd, Sr isotope and trace element systematics of the Pitcairn hotspot. *Earth Planet. Sci. Lett.* **196**, 197–212 (2002).
218. Castillo, P. R. The recycling of marine carbonates and sources of HIMU and FOZO ocean island basalts. *Lithos* **216**, 254–263 (2015).
219. Niu, Y. L. & O'Hara, M. J. Origin of ocean island basalts: A new perspective from petrology, geochemistry, and mineral physics considerations. *J. Geophys. Res. Solid Earth* **108**, 2209 (2003).
220. Pilet, S., Baker, M. B. & Stolper, E. M. Metasomatized lithosphere and the origin of alkaline lavas. *Science* **320**, 916–919 (2008).
221. Weiss, Y., Class, C., Goldstein, S. L. & Hanyu, T. Key new pieces of the HIMU puzzle from olivines and diamond inclusions. *Nature* **537**, 666–670 (2016).
222. McKenzie, D. & O'Nions, R. K. The source regions of ocean island basalts. *J. Petrol.* **36**, 133–159 (1995).
223. Collerson, K. D., Williams, Q., Ewart, A. E. & Murphy, D. T. Origin of HIMU and EM-1 domains sampled by ocean island basalts, kimberlites and carbonatites: The role of CO_2-fluxed lower mantle melting in thermochemical upwellings. *Phys. Earth Planet. Inter.* **181**, 112–131 (2010).
224. Hauri, E. H. Major-element variability in the Hawaiian mantle plume. *Nature* **382**, 415–419 (1996).
225. Prytulak, J. & Elliott, T. TiO_2 enrichment in ocean island basalts. *Earth Planet. Sci. Lett.* **263**, 388–403 (2007).
226. Sobolev, A. V., Hofmann, A. W., Sobolev, S. V. & Nikogosian, I. K. An olivine-free mantle source of Hawaiian shield basalts. *Nature* **434**, 590–597 (2005).
227. Delavault, H., Chauvel, C., Thomassot, E., Devey, C. W. & Dazas, B. Sulfur and lead isotopic evidence of relic Archean sediments in the Pitcairn mantle plume. *Proc. Natl Acad. Sci. USA* **113**, 12952–12956 (2016).
228. Farquhar, J. et al. Mass-independent sulfur of inclusions in diamond and sulfur recycling on early Earth. *Science* **298**, 2369–2372 (2002).
229. Gülcher, A. J. P., Gebhardt, D. J., Ballmer, M. D. & Tackley, P. J. Variable dynamic styles of primordial heterogeneity preservation in the Earth's lower mantle. *Earth Planet. Sci. Lett.* **536**, 116160 (2020).
230. Deschamps, F., Kaminski, E. & Tackley, P. J. A deep mantle origin for the primitive signature of ocean island basalt. *Nat. Geosci.* **4**, 879–882 (2011).
231. Graham, D. W. et al. Mantle source provinces beneath the northwestern USA delimited by helium isotopes in young basalts. *J. Volcanol. Geotherm. Res.* **188**, 128–140 (2009).
232. Castillo, P. The dupal anomaly as a trace of the upwelling lower mantle. *Nature* **336**, 667–670 (1988).
233. Jackson, M. G., Becker, T. W. & Konter, J. G. Evidence for a deep mantle source for EM and HIMU domains from integrated geochemical and geophysical constraints. *Earth Planet. Sci. Lett.* **484**, 154–167 (2018).
234. Hart, S. R. A large-scale isotope anomaly in the Southern Hemisphere mantle. *Nature* **309**, 753–757 (1984).
235. Hofmann, A. W. in *Treatise on Geochemistry* Vol. 2 (eds Holland, H. D. & Turekian, K. K.) 1–44 (Pergamon, 2007).
236. Warren, J. M. Global variations in abyssal peridotite compositions. *Lithos* **248**, 193–219 (2016).
237. Doucet, L. S. et al. Coupled supercontinent–mantle plume events evidenced by oceanic plume record. *Geology* **48**, 159–163 (2020).
238. Li, M., McNamara, A. K., Garnero, E. J. & Yu, S. Compositionally-distinct ultra-low velocity zones on Earth's core-mantle boundary. *Nat. Commun.* **8**, 177 (2017).
239. Jackson, M. G. et al. Ancient helium and tungsten isotopic signatures preserved in mantle domains least modified by crustal recycling. *Proc. Natl Acad. Sci. USA* **117**, 30993–31001 (2020).
240. Hieronymus, C. F. & Bercovici, D. Discrete alternating hotspot islands formed by interaction of magma transport and lithospheric flexure. *Nature* **397**, 604–607 (1999).
241. Jones, T. D. et al. The concurrent emergence and causes of double volcanic hotspot tracks on the Pacific plate. *Nature* **545**, 472–476 (2017).
242. Tatsumoto, M. Isotopic composition of lead in oceanic basalt and its implication to mantle evolution. *Earth Planet. Sci. Lett.* **38**, 63–87 (1978).
243. Dana, J. D. in *United States Exploring Expedition (with Atlas)* Vol. 10 (ed. Wilkes, C.) (Putnam, 1849).
244. Barker, A. K., Holm, P. M., Peate, D. W. & Baker, J. A. A 5 million year record of compositional variations in mantle sources to magmatism on Santiago, southern Cape Verde archipelago. *Contrib. Mineral. Petrol.* **160**, 133–154 (2010).
245. Harpp, K. S., Hall, P. S. & Jackson, M. G. Galápagos and Easter: A tale of two hotspots. *Galapagos Nat. Lab. Earth Sci.* **204**, 27–40 (2014).
246. Chauvel, C. et al. The size of plume heterogeneities constrained by Marquesas isotopic stripes. *Geochem. Geophys. Geosyst.* **13**, Q07005 (2012).
247. Koppers, A. A. P. et al. Age systematics of two young en echelon Samoan volcanic trails. *Geochem. Geophys. Geosyst.* **12**, Q07025 (2011).
248. Finlayson, V. A. et al. Sr–Pb–Nd–Hf isotopes and $^{40}Ar/^{39}Ar$ ages reveal a Hawaii–Emperor-style bend in the Rurutu hotspot. *Earth Planet. Sci. Lett.* **500**, 168–179 (2018).
249. Werner, R., Hoernle, K., Barckhausen, U. & Hauff, F. Geodynamic evolution of the Galápagos hot spot system (Central East Pacific) over the past 20 m.y.: Constraints from morphology, geochemistry, and magnetic anomalies. *Geochem. Geophys. Geosyst.* **4**, 1108 (2003).
250. Payne, J. A., Jackson, M. G. & Hall, P. S. Parallel volcano trends and geochemical asymmetry of the Society Islands hotspot track. *Geology* **41**, 19–22 (2013).
251. Ren, Z. Y., Ingle, S., Takahashi, E., Hirano, N. & Hirata, T. The chemical structure of the Hawaiian mantle plume. *Nature* **436**, 837–840 (2005).
252. Frey, F. A. & Rhodes, J. M. Intershield geochemical differences among Hawaiian volcanoes: Implications for source compositions, melting process and magma ascent paths. *Philos. Trans. R. Soc. A Math. Phys. Eng. Sci.* **342**, 121–136 (1993).
253. Kurz, M. D., Kenna, T. C., Lassiter, J. C. & DePaolo, D. J. Helium isotopic evolution of Mauna Kea volcano: First results from the 1-km drill core. *J. Geophys. Res. Solid Earth* **101**, 11781–11791 (1996).
254. DePaolo, D. J., Bryce, J. G., Dodson, A., Shuster, D. L. & Kennedy, B. M. Isotopic evolution of Mauna Loa and the chemical structure of the Hawaiian plume. *Geochem. Geophys. Geosyst.* **2**, 2000GC000139 (2001).
255. Konrad, K., Graham, D. W., Kent, A. J. R. & Koppers, A. A. P. Spatial and temporal variability in Marquesas Islands volcanism revealed by $^{3}He/^{4}He$ and the composition of olivine-hosted melt inclusions. *Chem. Geol.* **477**, 161–176 (2018).
256. Ito, G. & Mahoney, J. J. Flow and melting of a heterogeneous mantle: 2. Implications for a chemically nonlayered mantle. *Earth Planet. Sci. Lett.* **230**, 47–63 (2005).
257. Bryce, J. G., DePaolo, D. J. & Lassiter, J. C. Geochemical structure of the Hawaiian plume: Sr, Nd, and Os isotopes in the 2.8 km HSDP-2 section of Mauna Kea volcano. *Geochem. Geophys. Geosyst.* **6**, Q09G18 (2005).
258. Hofmann, A. W., Farnetani, C. G., Spiegelman, M. & Class, C. Displaced helium and carbon in the Hawaiian plume. *Earth Planet. Sci. Lett.* **312**, 226–236 (2011).
259. Harpp, K. S. & Weis, D. Insights into the origins and compositions of mantle plumes: A comparison of Galápagos and Hawai'i. *Geochem. Geophys. Geosyst.* **21**, e2019GC008887 (2020).
260. Weis, D., Harrison, L. N., McMillan, R. & Williamson, N. M. B. Fine-scale structure of Earth's deep mantle resolved through statistical analysis of Hawaiian basalt geochemistry. *Geochem. Geophys. Geosystems* **21**, e2020GC009292 (2020).
261. Nobre Silva, I. G., Weis, D. & Scoates, J. S. Isotopic systematics of the early Mauna Kea shield phase and insight into the deep mantle beneath the Pacific Ocean. *Geochem. Geophys. Geosyst.* **14**, 659–676 (2013).
262. Regelous, M., Hofmann, A. W., Abouchami, W. & Galer, S. J. G. Geochemistry of lavas from the Emperor Seamounts, and the geochemical evolution of Hawaiian magmatism from 85 to 42 Ma. *J. Petrol.* **44**, 113–140 (2003).
263. Harrison, L. N., Weis, D. & Garcia, M. O. The link between Hawaiian mantle plume composition, magmatic flux, and deep mantle geodynamics. *Earth Planet. Sci. Lett.* **463**, 298–309 (2017).
264. Williamson, N. M. B., Weis, D., Scoates, J. S., Pelletier, H. & Garcia, M. O. Tracking the geochemical transition between the Kea-dominated Northwest Hawaiian Ridge and the bilateral Loa-Kea trends of the Hawaiian Islands. *Geochem. Geophys. Geosyst.* **20**, 4354–4369 (2019).
265. Minster, J. B. & Jordan, T. H. Present-day plate motions. *J. Geophys. Res.* **83**, 5331–5354 (1978).
266. Müller, R. D., Royer, J. Y. & Lawver, L. A. Revised plate motions relative to the hotspots from combined Atlantic and Indian Ocean hotspot tracks. *Geology* **21**, 275–278 (1993).
267. Duncan, R. A. & Clague, D. A. in *The Ocean Basins and Margins Vol. 7A: The Pacific Ocean* (eds Nairn, A. E. M., Stehli, F. L., & Uyeda, S.) 89–121 (Plenum Press, 1985).
268. Wessel, P. & Kroenke, L. W. Pacific absolute plate motion since 145 Ma: An assessment of the fixed hot spot hypothesis. *J. Geophys. Res. Solid Earth* **113**, B06101 (2008).
269. Wessel, P. & Conrad, C. P. Assessing models for Pacific absolute plate and plume motions. *Geochem. Geophys. Geosyst.* **20**, 6016–6032 (2019).
270. Tarduno, J. A. et al. The Emperor Seamounts: Southward motion of the Hawaiian hotspot plume in Earth's mantle. *Science* **301**, 1064–1069 (2003).
271. Tarduno, J. A. & Koppers, A. A. P. When hotspots move the new view of mantle dynamics made possible by scientific ocean drilling. *Oceanography* **32**, 150–152 (2019).
272. O'Connor, J. M. et al. Constraints on past plate and mantle motion from new ages for the Hawaiian-Emperor Seamount Chain. *Geochem. Geophys. Geosyst.* **14**, 4564–4584 (2013).
273. Koppers, A. A. P. et al. New $^{40}Ar/^{39}Ar$ age progression for the Louisville hot spot trail and implications for inter–hot spot motion. *Geochem. Geophys. Geosyst.* **12**, Q0AM02 (2011).
274. Sharp, W. D. & Clague, D. A. 50-Ma initiation of Hawaiian-Emperor bend records major change in Pacific plate motion. *Science* **313**, 1281–1284 (2006).
275. Bono, R. K., Tarduno, J. A. & Bunge, H. P. Hotspot motion caused the Hawaiian-Emperor Bend and LLSVPs are not fixed. *Nat. Commun.* **10**, 3370 (2019).
276. Hassan, R., Muller, R. D., Gurnis, M., Williams, S. E. & Flament, N. A rapid burst in hotspot motion through the interaction of tectonics and deep mantle flow. *Nature* **533**, 239–242 (2016).
277. Arnould, M., Ganne, J., Coltice, N. & Feng, X. Northward drift of the Azores plume in the Earth's mantle. *Nat. Commun.* **10**, 3235 (2019).
278. Wang, S. M., Yu, H. Z., Zhang, Q. & Zhao, Y. H. Absolute plate motions relative to deep mantle plumes. *Earth Planet. Sci. Lett.* **490**, 88–99 (2018).
279. Morgan, W. J. & Morgan, J. P. in *Plates, Plumes and Planetary Processes* Vol. 430 (eds Foulger, G. R. & Jurdy, D. M.) 65–78 (Geological Society of America, 2007).
280. Tetley, M. G., Williams, S. E., Gurnis, M., Flament, N. & Muller, R. D. Constraining absolute plate motions since the Triassic. *J. Geophys. Res. Solid Earth* **124**, 7231–7258 (2019).
281. Becker, T. W., Schaeffer, A. J., Lebedev, S. & Conrad, C. P. Toward a generalized plate motion reference frame. *Geophys. Res. Lett.* **42**, 3188–3196 (2015).
282. Wang, C. Z., Gordon, R. G., Zhang, T. & Zheng, L. Observational test of the global moving hot spot reference frame. *Geophys. Res. Lett.* **46**, 8031–8038 (2019).

283. Doubrovine, P. V., Steinberger, B. & Torsvik, T. H. Absolute plate motions in a reference frame defined by moving hot spots in the Pacific, Atlantic, and Indian oceans. *J. Geophys. Res. Solid Earth* **117**, B09101 (2012).
284. Burke, K. & Dewey, J. F. Plume-generated triple junctions: key indicators in applying plate tectonics to old rocks. *J. Geol.* **81**, 406–433 (1973).
285. Fahrig, W. F. & Schwarz, E. J. Additional paleomagnetic data on the Baffin diabase dikes and a revised franklin pole. *Can. J. Earth Sci.* **10**, 576–581 (1973).
286. Brune, S., Williams, S. E., Butterworth, N. P. & Muller, R. D. Abrupt plate accelerations shape rifted continental margins. *Nature* **536**, 201–204 (2016).
287. Bercovici, D. & Long, M. D. Slab rollback instability and supercontinent dispersal. *Geophys. Res. Lett.* **41**, 6659–6666 (2014).
288. Huang, C. et al. Modeling the inception of supercontinent breakup: stress state and the importance of orogens. *Geochem. Geophys. Geosyst.* **20**, 4830–4848 (2019).
289. Ziegler, P. A. & Cloetingh, S. Dynamic processes controlling evolution of rifted basins. *Earth Sci. Rev.* **64**, 1–50 (2004).
290. Buiter, S. J. H. & Torsvik, T. H. A review of Wilson Cycle plate margins: A role for mantle plumes in continental break-up along sutures? *Gondwana Res.* **26**, 627–653 (2014).
291. Brune, S., Popov, A. A. & Sobolev, S. V. Quantifying the thermo-mechanical impact of plume arrival on continental break-up. *Tectonophysics* **604**, 51–59 (2013).
292. Dang, Z. et al. Weak orogenic lithosphere guides the pattern of plume-triggered supercontinent break-up. *Commun. Earth Environ.* **1**, 51 (2020).
293. Koptev, A., Calais, E., Burov, E., Leroy, S. & Gerya, T. Dual continental rift systems generated by plume–lithosphere interaction. *Nat. Geosci.* **8**, 388–392 (2015).
294. Whittaker, J. M. et al. Eastern Indian Ocean microcontinent formation driven by plate motion changes. *Earth Planet. Sci. Lett.* **454**, 203–212 (2016).
295. Gaina, C., Gernigon, L. & Ball, P. Palaeocene–Recent plate boundaries in the NE Atlantic and the formation of the Jan Mayen microcontinent. *J. Geol. Soc.* **166**, 601–616 (2009).
296. Nemčok, M. et al. Mechanisms of microcontinent release associated with wrenching-involved continental break-up; a review. *Geol. Society Publ.* **431**, 323–359 (2016).
297. Müller, D. R., Gaina, C., Roest, W. R. & Hansen, D. L. A recipe for microcontinent formation. *Geology* **29**, 203–206 (2001).
298. Albarède, F. The growth of continental crust. *Tectonophysics* **296**, 1–14 (1998).
299. Van Kranendonk, M. J. Two types of Archean continental crust: Plume and plate tectonics on early Earth. *Am. J. Sci.* **310**, 1187–1209 (2011).
300. Reagan, M. K. et al. Forearc ages reveal extensive short-lived and rapid seafloor spreading following subduction initiation. *Earth Planet. Sci. Lett.* **506**, 520–529 (2019).
301. Rey, P. F., Coltice, N. & Flament, N. Spreading continents kick-started plate tectonics. *Nature* **513**, 405–408 (2014).
302. Maunder, B., Prytulak, J., Goes, S. & Reagan, M. Rapid subduction initiation and magmatism in the Western Pacific driven by internal vertical forces. *Nat. Commun.* **11**, 1874 (2020).
303. Gerya, T. V., Stern, R. J., Baes, M., Sobolev, S. V. & Whattam, S. A. Plate tectonics on the Earth triggered by plume-induced subduction initiation. *Nature* **527**, 221–225 (2015).
304. Arnould, M., Coltice, N., Flament, N. & Mallard, C. Plate tectonics and mantle controls on plume dynamics. *Earth Planet. Sci. Lett.* **547**, 116439 (2020).
305. Tackley, P. J. Modelling compressible mantle convection with large viscosity contrasts in a three-dimensional spherical shell using the yin-yang grid. *Phys. Earth Planet. Inter.* **171**, 7–18 (2008).
306. Faccenna, C. et al. Subduction-triggered magmatic pulses: A new class of plumes? *Earth Planet. Sci. Lett.* **299**, 54–68 (2010).
307. Sager, W. W. et al. Oceanic plateau formation by seafloor spreading implied by Tamu Massif magnetic anomalies. *Nat. Geosci.* **12**, 661–66 (2019).
308. Sager, W. W. et al. An immense shield volcano within the Shatsky Rise oceanic plateau, northwest Pacific Ocean. *Nat. Geosci.* **6**, 976–981 (2013).
309. Conrad, C. P. & Lithgow-Bertelloni, C. Faster seafloor spreading and lithosphere production during the mid-Cenozoic. *Geology* **35**, 29–32 (2007).
310. Müller, R. D., Sdrolias, M., Gaina, C. & Roest, W. R. Age, spreading rates, and spreading asymmetry of the world's ocean crust. *Geochem. Geophys Geosystems* **9**, Q04006 (2008).
311. Jackson, C. R. M., Bennett, N. R., Du, Z., Cottrell, E. & Fei, Y. Early episodes of high-pressure core formation preserved in plume mantle. *Nature* **553**, 491–495 (2018).
312. Conrad, C. P., Lithgow-Bertelloni, C. & Louden, K. E. Iceland, the Farallon slab, and dynamic topography of the North Atlantic. *Geology* **32**, 177–180 (2004).
313. Steinberger, B., Conrad, C. P., Tutu, A. O. & Hoggard, M. J. On the amplitude of dynamic topography at spherical harmonic degree two. *Tectonophysics* **760**, 221–228 (2019).
314. Li, Z. X. & Zhong, S. J. Supercontinent–superplume coupling, true polar wander and plume mobility: Plate dominance in whole-mantle tectonics. *Phys. Earth Planet. Inter.* **176**, 143–156 (2009).
315. Petersen, K. D., Nielsen, S. B., Clausen, O. R., Stephenson, R. & Gerya, T. Small-scale mantle convection produces stratigraphic sequences in sedimentary basins. *Science* **329**, 827–830 (2010).
316. Rovere, A. et al. Mid-Pliocene shorelines of the US Atlantic Coastal Plain — An improved elevation database with comparison to Earth model predictions. *Earth Sci. Rev.* **145**, 117–131 (2015).
317. Muller, R. D. Sedimentary basins feeling the heat from below. *Science* **329**, 769–770 (2010).
318. Schoene, B. et al. U-Pb constraints on pulsed eruption of the Deccan Traps across the end-Cretaceous mass extinction. *Science* **363**, 862–866 (2019).
319. Hull, P. M. et al. On impact and volcanism across the Cretaceous-Paleogene boundary. *Science* **367**, 266–272 (2020).
320. Sprain, C. J. et al. The eruptive tempo of Deccan volcanism in relation to the Cretaceous-Paleogene boundary. *Science* **363**, 866–870 (2019).
321. Reichow, M. K. et al. The timing and extent of the eruption of the Siberian Traps large igneous province: Implications for the end-Permian environmental crisis. *Earth Planet. Sci. Lett.* **277**, 9–20 (2009).
322. Burgess, S. D. & Bowring, S. A. High-precision geochronology confirms voluminous magmatism before, during, and after Earth's most severe extinction. *Sci. Adv.* **1**, e1500470 (2015).
323. Clapham, M. E. & Renne, P. R. Flood basalts and mass extinctions. *Annu. Rev. Earth Planet. Sci.* **47**, 275–27 (2019).
324. Sobolev, S. V. et al. Linking mantle plumes, large igneous provinces and environmental catastrophes. *Nature* **477**, 312–316 (2011).
325. Payne, J. L. & Clapham, M. E. End-Permian mass extinction in the oceans: an ancient analog for the twenty-first century? *Annu. Rev. Earth Planet. Sci.* **40**, 89–111 (2012).
326. Renne, P. R. et al. State shift in Deccan volcanism at the Cretaceous-Paleogene boundary, possibly induced by impact. *Science* **350**, 76–78 (2015).
327. French, S. W. & Romanowicz, B. A. Whole-mantle radially anisotropic shear velocity structure from spectral-element waveform tomography. *Geophys. J. Int.* **199**, 1303–1327 (2014).
328. Touboul, M., Puchtel, I. S. & Walker, R. J. ^{182}W evidence for long-term preservation of early mantle differentiation products. *Science* **335**, 1065–1069 (2012).
329. Norton, I. O. Plate motions in the North Pacific: the 43 Ma nonevent. *Tectonics* **14**, 1080–1094 (1995).
330. Tarduno, J. A. & Cottrell, R. D. Paleomagnetic evidence for motion of the Hawaiian hotspot during formation of the Emperor seamounts. *Earth Planet. Sci. Lett.* **153**, 171–180 (1997).
331. Torsvik, T. H. et al. Pacific plate motion change caused the Hawaiian-Emperor Bend. *Nat. Commun.* **8**, 15660 (2017).
332. Steinberger, B., Sutherland, R. & O'Connell, R. J. Prediction of Emperor-Hawaii seamount locations from a revised model of global plate motion and mantle flow. *Nature* **430**, 167–173 (2004).
333. Matthews, K. J. et al. Global plate boundary evolution and kinematics since the late Paleozoic. *Glob. Planet. Change* **146**, 226–250 (2016).
334. Seton, M. et al. Global continental and ocean basin reconstructions since 200 Ma. *Earth Sci. Rev.* **113**, 212–270 (2012).
335. Besse, J. & Courtillot, V. Apparent and true polar wander and the geometry of the geomagnetic field over the last 200 Myr. *J. Geophys. Res. Solid Earth* **107**, EPM 6-1–EPM 6-31 (2002).
336. Torsvik, T. H. et al. Phanerozoic polar wander, palaeogeography and dynamics. *Earth Sci. Rev.* **114**, 325–368 (2012).
337. Gold, T. Instability of the Earth's axis of rotation. *Nature* **175**, 526–529 (1955).
338. Steinberger, B. & O'Connell, R. J. Changes of the Earth's rotation axis owing to advection of mantle density heterogeneities. *Nature* **387**, 169–173 (1997).
339. Dziewonski, A. M., Lekic, V. & Romanowicz, B. A. Mantle anchor structure: an argument for bottom up tectonics. *Earth Planet. Sci. Lett.* **299**, 69–79 (2010).
340. Creveling, J. R., Mitrovica, J. X., Chan, N.-H., Latychev, K. & Matsuyama, I. Mechanisms for oscillatory true polar wander. *Nature* **491**, 244–248 (2012).
341. Steinberger, B., Seidel, M. L. & Torsvik, T. H. Limited true polar wander as evidence that Earth's nonhydrostatic shape is persistently triaxial. *Geophys. Res. Lett.* **44**, 827–834 (2017).
342. Mitchell, R. N et al. A Late Cretaceous true polar wander oscillation. *Nat. Commun.* https://doi.org/10.1038/s41467-021-23803-8 (2020).
343. Sager, W. W. & Koppers, A. A. P. Late Cretaceous polar wander of the Pacific plate: Evidence of a rapid true polar wander event. *Science* **287**, 455–459 (2000).
344. Woodworth, D. & Gordon, R. G. Paleolatitude of the Hawaiian hot spot since 48 Ma: evidence for a mid-Cenozoic true polar stillstand followed by late Cenozoic true polar wander coincident with Northern Hemisphere glaciation. *Geophys. Res. Lett.* **45**, 11632–11640 (2018).

Acknowledgements
The authors are supported by the National Science Foundation (NSF) grants OCE-1912932 (A.A.P.K., K.K.), EAR-1900652 (M.G.J.) and EAR-1758198 (B.R.); National Aeronautics and Space Administration (NASA) grant OSP 201601412-001 (T.W.B.); Centre of Excellence project 223272 through the Research Council of Norway (RCN) and the innovation pool of the Helmholtz Association via an "Advanced Earth System Modelling Capacity (ESM)" activity (B.S.); and Australian Research Council (ARC) grant IH130200012 (R.D.M.). We thank E. Garnero and T. Jones for informal discussions that improved the manuscript.

Author contributions
The authors contributed equally to all aspects of the article.

Competing interests
The authors declare no competing interests.

Peer review information
Nature Reviews Earth & Environment thanks D. Weis (who co-reviewed with N. Williamson), Y. Niu, A. Hofmann and J. Ritsema for their contribution to the peer review of this work.

Publisher's note
Springer Nature remains neutral with regard to jurisdictional claims in published maps and institutional affiliations.

Supplementary information
The online version contains supplementary material available at https://doi.org/10.1038/s43017-021-00168-6.